MRU Cardington Technical Note No. 12

Orientation calculations for the Cardington turbulence probe

by

A.J. Lapworth

17 May 1993

Met. Office Research Unit
RAF Cardington
Shortstown
Beds, MK42 0TH

MRU CARDINGTON

MRU Cardington Technical Note No. 12

Orientation calculations for the Cardington turbulence probe

by

A.J.Lapworth

17 May 1993

Met. Office Research Unit
RAF Cardington
Shortstown
Beds, MK42 0TH

Note

This paper has not been published and PMetO(Cardington) should be consulted before quoting from it.

Orientation calculations for the Cardington turbulence probe

A.J. Lapworth

Contents

Orientation calculations for the Cardington turbulence probe

A.J. Lapworth

17 May 1993

Abstract

This note is a reference for the calculation of orientations which has been standard on the Cardington turbulence probe from about 1984. The design of the probe is briefly discussed, plus some results. Some additional notes have been added on correcting an ambiguity which arises when the cable is laid back towards the south.

1 Introduction

The 'new' Cardington turbulence probe was designed and developed during the Mason era, in the period 1981-1984, by members of the Meteorological Research Unit at Cardington. It is a balloon mounted instrument consisting of three Gill propeller anemometers rigidly attached to a three-magnetometer set and two inclinometers mounted at right angles to each other. A pressure sensor, and temperature and humidity sensors are included.

The outputs are telemetered to the ground and stored on magnetic disc. The data processing routines then use algorithms based on results derived in this note to determine the mean wind and turbulence quantities.

In this note the probe is described and features of the spectra obtained with it discussed. A formula is derived for converting the Gill outputs into instantaneous winds relative to orthogonal axes fixed relative to the probe. This is followed by a short discussion on the orientation problem. The transformation matrix is then calculated to determine the winds relative to a ground based system. Finally the rotations necessary to align the components into the mean wind are given.

In the next two sections the angle of dip is calculated from the probe outputs and a diagnostic result is derived using the inclinometer outputs together with separate Gill readings.

An approximate method of determining the translational motions of the probe using only probe derived information is described, and finally a method of combining the angles obtained by this calculation with a new transformation to remove the effect of inclinometer accelerations is given.

2 Probe description

The new Cardington turbulence probe consists of a package freely rotating and balanced about the balloon cable as an axis, and constrained to point roughly into the mean wind by a vertical vane separated by a tubular boom from the probe body.

Three Gill propeller anemometers are mounted on the wind-ward face of the package, their axes lying at 120° intervals on the surface of a cone with a 30° half angle and its own axis drooped by 20° from the probe horizontal. The Gills are symmetrically positioned with one uppermost, one to port and the other to starboard. The vane keeps the mean wind within the Gill cone for motions having a length scale greater than ten metres and is separated from the body in order to avoid distortion of the up-wind flow by the tail and to give leverage. The Gills are drooped as the balloon cable tends to lie back in a wind, and as updraughts are stronger than downdraughts in convective situations. The bearings about the cable axis are designed to avoid rattle and allow free rotation.

Two inclinometers are mounted as close to the cable as possible in order to minimise accelerations due to probe rotational motions. Both inclinometers measure the component of gravity perpendicular to a given axis in a specific plane, one being oriented to detect pitching motions, the other to detect rolling motions. These instruments are affected by accelerations other than gravity and are electronically filtered with a time constant of two seconds to remove spurious, vibration-induced signals. A three axis magnetometer is used to measure yawing motions and great care has to be taken to mount this in a position remote from magnetic effects due to the probe itself. A three axis rather than two axis device is used in order to allow the total field and dip angle to be calculated as these may vary due to local effects.

Also included in the package are a pressure transducer, a platinum resistance thermometer for high frequency temperature measurements, and dry and wet bulb thermistors with long term stability. The thermistors are mounted in a downward facing radiation shield and are aspirated by a fan. The probe is earthed by a brush to the cable to avoid the effects of static discharge on the CMOS logic. Care is taken to secure all parts mechanically to aircraft standards, with redundant fittings as the package is heavy and operates at heights of over a mile up.

The probe analogue outputs are digitised, Manchester encoded, and transmitted to a ground receiver where the data is decoded and stored by a PDP 11/34 computer on magnetic disc.

3 Spectra obtained with the new turbulence probe

The spectra obtained from the turbulence probe are affected by several sources of error. However the errors can be minimised by optimising the processing algorithm provided their sources are understood. A series of tests with the probe mounted on a fixed mast or a balloon at 20 metres and above and intercompared with a sonic anemometer gave the following results. On a fixed mast the spectra compare well with those of the sonic apart from a small peak in the $V^{2'}$ spectra at around 10 metres and a drop off in frequency response below a wavelength of $\sim$ 10 metres due to the inherent limitations of the Gills, The frequency fall-off is greater if the Gills are set at larger angles to the mean wind.

The $V^{2'}$ spectra peak is at the length constant of the probe and is most probably due to phase lags between the Gills and main vane in the region of the spectrum where their contributions overlap. Experiments with Gill extensions indicated that the peak was probably not an upwind effect of the probe body or the tail. The effect is worse close to the ground where the energy in this part of the spectrum is enhanced and is sensitive to errors in the measured cosine response.

The spectra of the inclinometers show three peaks when mounted on the balloon cable at heights up to $\sim$ 100 feet. The main peak is at wavelengths greater than $\sim$ 70 metres and is due to balloon motions. There is a secondary peak at 10 - 15 metres (ie. a period of 2-3 seconds) which is mainly due to a transverse vibration of the balloon cable excited by the mass of the probe. This peak unfortunately overlaps with "real" affects due to turbulence motions on the probe and thus simple filtering of the inclinometers at this wavelength not only removes the spurious peak in the spectra due to the transverse vibrations but also increases the peak at $\sim$ 10 metres as a result of removing "real" inclinometer information. A third peak in the inclinometer spectra at the shortest wavelength is probably due to the cable buzzing as a result of eddy shedding induced vibration in the wind. This can be safely filtered out of the inclinometers at wavelengths shorter than $\sim$ 5 metres. At increased height the peaks shift to longer wavelengths. The transverse vibration peak(s) increases in wavelength as $\sim L$ (L is the cable length), while the peak due to balloon 'inverse pendulum' motions increases as $\sim L^{\frac{1}{2}}$. Thus they become less well separated as L increases, and the filter period has to be increased. Over the balloon height range of 500 to 5000 feet the period of transverse vibrations varies from 2 to 25 seconds while the balloon motion period varies from 20 to 75 seconds. The filter period is best set to half the balloon motion period.

The spectra are significantly affected by translational effects due to balloon motions at heights greater than $\sim$ 100 feet. The translational motions have wavelengths in the range 70 metres to several kilometres and give significant peaks in the $V^{2'}$ spectra. These amount to an increase in $v^{2'}$ energy of $\sim$ 50% at 500 feet increasing by $\sim$ 100% per 1000 feet in medium conditions. The $u^{2'}$ spectra also acquires some energy due to translational motions (about 10% at 500 feet, increasing by $\sim$ 20% per 1000 feet), while the $w^{2'}$ spectra is nearly unaffected. A method of removing the translational energy from the spectra that appears fairly successful is to use the inclinometer and magnetometer information to determine azimuth and declination angles. These angles can then be used to determine the position assuming a straight line approximation to the balloon cable, and the coordinates of the position filtered with a time constant of 10 - 15 seconds before differentiating to determine the translational velocities. This simple approximation works very well up to $\sim$ 500 feet and appears to give beneficial corrections to much greater heights, the errors in $v^{2'}$ increasing by $\sim$ 50% to 100% per 2000 feet. Above $\sim$ 500 feet the filter time constant has to be increased as the wavelength due to balloon motion increases and the transverse vibration mode of the cable predominates at 60 - 100 metres. At 2000 feet a suitable time constant is $\sim$ 20 seconds.

An extension of this procedure (suggested by P.J. Mason) can be used to remove the effects of spurious (non-gravitational) accelerations on the inclinometers on the spectra. These accelerations are proportional to the square of the frequency, and become significant at frequencies greater than 0·1 Hz (corresponding to $\sim$ 50 metres). The peak in the inclinometer spectra at 0·3 to 0·5 Hz (15 - 10 metres) is mainly due to these accelerations but as has been mentioned above, simple filtering of the inclinometer affects the "real" spectra and would also affect calculations of translational motion. A solution to this is to use the azimuth (m) and declination (n) angles previously computed. The combined functions $\sin m$, $\cos n$ and $\sin m$, $\sin n$ are quantities that only vary at wavelengths greater than $\sim$ 70 metres and can thus be filtered at shorter wavelengths. After filtering, m and n can be recalculated and used to determine turbulence quantities. It should be noted that direct filtering of m corrupts the data as it contains high frequency components with "real" information.

The $v^{2'}$ spectra processed using this technique still show a peak in the 10 - 200 metre region. The wavelength of the peak varies with height and is seen in the magnetometer spectra. It may be partly due to the affects associated with the length constant of the probe mentioned previously, but is probably mainly due to the "real" affect of the transverse vibration mode - ie. the fact that air is moving relative to the probe at this frequency. This cannot be simply allowed for with the tracking connection as the inclinometers are strongly affected by non-gravitational accelerations due to the same vibration. In addition, the motion is not simply related to orientation.

At increasing levels of turbulence ($u' \sim 1m/s$) the peaks in the $v^{2'}$ spectra tend to become relatively submerged. Conversely at low levels of turbulent energy ($\sim 0 \cdot 3\ m/s$) they are prominent.

Finally it should be noted that in strong winds and highly turbulent conditions the probe spectra become more and more affected by the enhanced cable motions.

Two other effects on the spectra have been considered. These are the accelerations of the inclinometers due to rotational motions of the probe about its axis and the translational affect on the Gills due to the same rotational motions. These both appear to be second order affects, especially if the inclinometers are close to the cable and if alignment of the Gill axes extends backwards through the cable.

4 Orientation calculations

4.1 Wind relative to probe axes X, Y, Z

First obtain velocity components relative to the right handed set X, Y, Z.

$$\sin q = \sin H \sin 30^\circ \tag{1}$$

$$\cos(90^\circ - q) = \sin H/2 \tag{2}$$

$$\sin p = \sin H \ \sin 60^\circ \tag{3}$$

$$\cos(90^\circ - p) = \sqrt{3} \sin H/2 \tag{4}$$

If X, Y, Z have velocity components u, v, w

$$\begin{aligned} -u_p &= u \cos H + v\sqrt{3} \sin H/2 - w \sin H/2 \\ -u_s &= u \cos H - v\sqrt{3} \sin H/2 - w \sin H/2 \\ -u_t &= u \cos H + w \sin H \end{aligned} \tag{5}$$

$$u = -\frac{1}{3 \cos H}(u_t + u_p + u_s) \tag{6}$$

$$v = -\frac{1}{\sqrt{3} \sin H}(u_p - u_s) \tag{7}$$

$$w = -\frac{1}{3 \sin H}(2u_t - u_p - u_s) \tag{8}$$

Anemometer components given as negative as their output is positive for velocities in towards the centre.

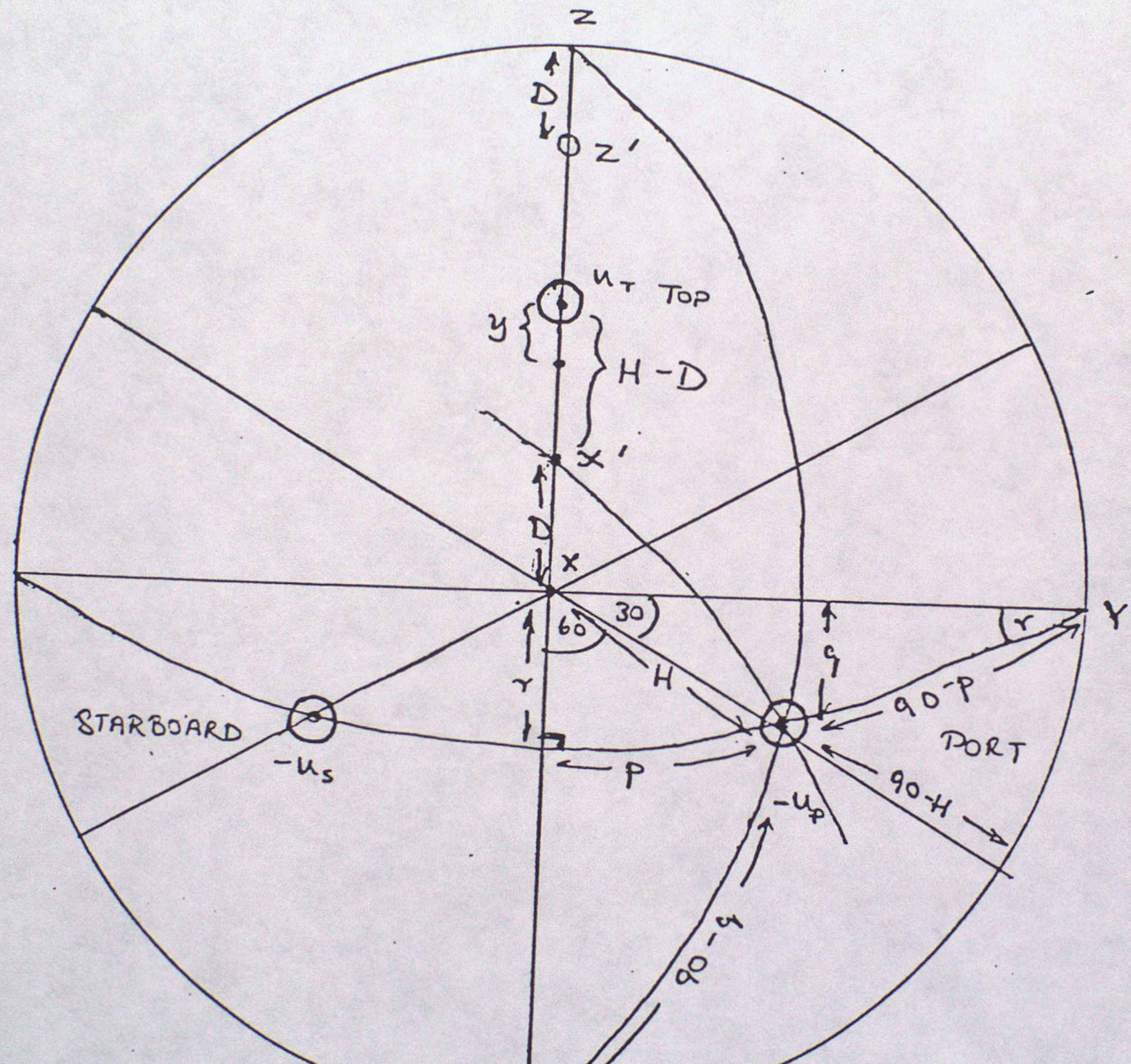

Figure 1: Gill stereogram, showing derivation of components of wind velocity relative to an orthogonal frame (North, West, Up) from readings of three cosine response anemometers mounted at 60° intervals on a cone of half angle H, with its axis tilted down by angle D from the horizontal.

The velocities are then measured relative to a set of axes X', Y', Z' tilted back to D to X, Y, Z.

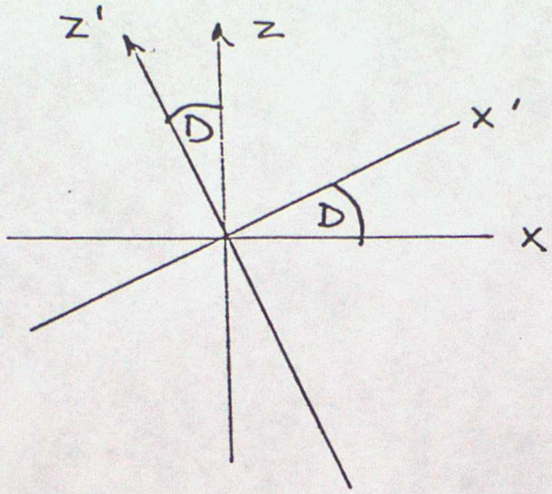

$$u' = u \cos D + w \sin D \tag{9}$$

$$w' = -u \sin D + w \cos D \tag{10}$$

$$v' = v \tag{11}$$

$$u = (\sin D/3 \sin H - \cos D/3 \cos H)(u_p + u_s) - (\cos D/3 \cos H + 2 \sin D/3 \sin H)u_t \tag{12}$$

$$v = (1/\sqrt{3} \sin H)(u_s - u_p) \tag{13}$$

$$w = (\cos D/3 \sin H + \sin D/3 \cos H)(u_p + u_s) + (\sin D/3 \cos H - 2 \cos D/3 \sin H)u_t \tag{14}$$

It is also useful to know the cosines of the angles between the anemometers and the x' direction.

(i) For u_t the angle is $H - D$, so Cosine$_t$ is $\cos(H - D)$ trivially.

(ii) For u_p (and u_s follows by analogy),

$$\sin(90° - p) = \sin(90° - H)/\sin(90° - r) \tag{15}$$

i.e.

$$\cos r = \cos H/\cos p \tag{16}$$

By similar reasoning, Cosine$_p$ is

$$\cos p \cos(r + D) = \cos p \cos\left(\cos^{-1}(\cos H/\cos p) + D\right) \tag{17}$$

5 Errors

The main error using Gill anemometers is in evaluating the deviation of the Gill from a cosine response. This deviation is worse and more prone to error at large angles. Correcting for the error involves an iterative procedure in the program in which an approximation to the true wind vector is made from the Gill outputs, and this is used with cosine error tables to determine the actual wind components along the Gills.

Experimental results appear to show that a symmetrical arrangement of Gills is better than a non-symmetrical layout, probably because errors in the cosine deviation then tend to cancel. An error analysis assuming known cosine deviations indicates $H \sim 54°44'$ gives minimum errors (ie. the Gills are orthogonal). However cosine deviation errors become quite large at these angles and $H \sim 30°$ appears satisfactory. In addition response time of the Gills falls off as a cosine and so is increased at high angles and starting errors (due to friction) become important.

6 Definition of a set of orthogonal co-ordinates by angular reference to two fixed axes

The problem of determining the orientation of a freely gymballed turbulence probe using inclinometers and magnetometers reduces to that of defining the orientation of an orthogonal set of axes (the turbulence probe) A, B and C if the direction cosines a, b, c these axes make respectively with a fixed direction G (gravity) and the direction cosines α, β, γ they make with another fixed direction M (the magnetic vector) are known.

In the general case, if a, b and c (or α, β, and γ) only are known, the set of axes is defined by *three* cones centred on G (or M). If the other three cosines, relative to M (or G) are known then three pairs of intersecting cones define, in general, two possible directions for each axes. However, only one of each pair of directions will combine to form the correct right handed set of probe axes. In fact, as will be seen, only five direction cosines are necessary and sufficient to define the probe orientation, and *if an additional piece of information, ie. that the probe does not invert, is introduced*, then only two cosines relative to each axis are necessary.

This is demonstrated in figure (1). The axis A makes direction cosine a with G and α with M. The axis B makes direction cosine b with G and with M. Thus A and B can take the orientations shown on the stereographic projection. However by reflection through the mirror plane containing G and M they can take the orientation A', B'. The sets A, B and A', B' define two *different* positions for the third axis, ie. C and C' which are related by an 180° rotation about the (diad) axis shown normal to the G, M plane. To distinguish between these two possible orientations of the third axis, it may be noted that one will always be below the plane of the unit circle — that is, the probe will be inverted. Alternatively, information from a fifth direction cosine relative to either G or M may be used.

The above results can be confirmed algebraically as follows. In the stereogram, the probe is shown with pitch θ, yaw ϕ and roll ρ. Gravity has strength g and the magnetic field M has components H_x and H_y along with x and negative z axes respectively. The magnetometers measure components α, β, γ along the probe axes A, B, C. These are related to H_x, H_y, ϕ, θ and ρ by the following three equations.

$$\alpha = H_z \sin\theta + H_x \cos\phi \cos\theta \tag{18}$$

$$\beta \cos\rho + \gamma \sin\rho = H_x \sin\phi \tag{19}$$

$$-\beta \sin\rho + \gamma \cos\rho = H_x \cos\phi \sin\theta - H_z \cos\theta \tag{20}$$

The inclinometers measure components perpendicular to their own axis, in the plane of their pendula. If three are used they could be mounted to give the three gravitational components a, b, c and A, B, C.

$$a = g \sin y \cos x = g \sin\theta \tag{21}$$

from triangle A in stereogram

$$b = g \cos\theta \sin\rho \tag{22}$$

$$c = -g \cos\theta \cos\rho \tag{23}$$

The magnetometer equations can be re-arranged to give:

$$\cos\phi = (\alpha - H_z \sin\theta)/H_x \cos\theta \tag{24}$$

$$\sin\phi = \frac{\beta \cos\theta + \alpha \sin\rho \sin\theta - H_z \sin\rho}{H_x \cos\rho \cos\theta} \tag{25}$$

for $0 < \phi < 360°$

The inclinometer equations give:

For $-90° < \theta < 90°$

$$\sin\theta = +a/g \qquad \cos\theta = \sqrt{1 - a^2/g^2} \tag{26}$$

For $-180° < \rho < 180°$

$$\sin\rho = b/\sqrt{g^2 - a^2} \quad \cos\rho = \pm\sqrt{(g^2 - a^2 - b^2)/(g^2 - a^2)} \tag{27}$$

If we restrict the probe to be upright, i.e. $-90° < \rho < 90°$, we can take the positive root for $\cos\rho$.

Combining the magnetometer and inclinometer equations

$$\cos\phi = \frac{g\alpha - H_z a}{H_x \sqrt{(g^2 - a^2)}} \tag{28}$$

$$\sin\phi = \frac{\beta(g^2 - a^2) + ab\alpha - H_z bg}{H_x\sqrt{(g^2 - a^2)(g^2 - a^2 - b^2)}} \tag{29}$$

Thus ϕ is uniquely determined, given only a, b, α and β. We can also use the identity $\sin^2\phi + \cos^2\phi = 1$ to determine the angle of dip. The inclinometer equations uniquely determined θ and ρ given only a and b provided $-90° < \rho < 90°$.

Another system was previously considered, in which ρ was constrained to be 0° — that is the probe pitch axis was kept gravitationally horizontal. This would have reduced the number of necessary inclinometers to one. However an error analysis showed that an error of 1° in maintaining $\rho = 0°$ gave up to 15° error in orientation of the probe and experiments using prototypes showed that ρ could be $\pm 5°$ or more in error. The present system does not show "error multiplication" of this type provided the cable axis is within 45° of the vertical.

Although only two magnetometers are strictly necessary, the values of H_x, H_z (or total H and angle of dip) need to be monitored as they vary with locality. As a result three magnetometers should be used, and this will give some much needed redundancy.

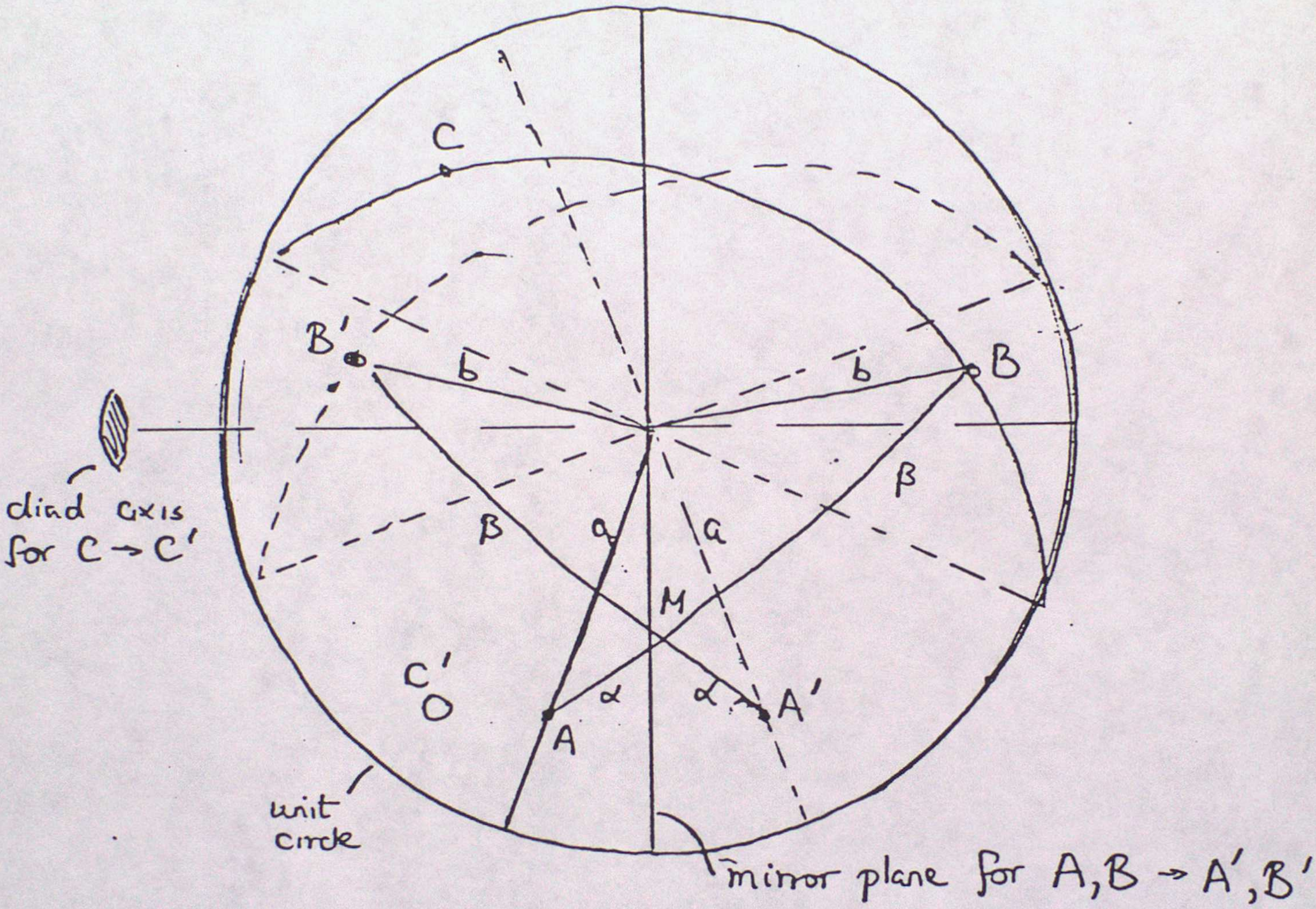

Figure 2: Stereographic projection. Dots show south pole projection (ie. vectors above plane) and circles north pole projection (ie. vectors below plane).

6.1 Rotating wind components

Required to determine wind components u, v, w relative to fixed axes x, y, z from u', v', w' relative to A, B, C.

This can be accomplished by three separate two-dimensional rotations — refer to Figure 3.

(i)

$$v_1 = v' \cos \rho + w' \sin \rho$$

$$w_1 = -v' \sin \rho + w' \cos \rho \tag{30}$$

$$u_1 = u'$$

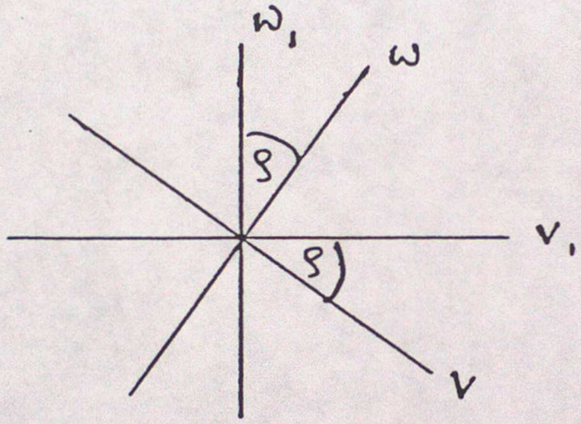

(ii)

$$u_2 = u_1 \cos \theta + w_1 \sin \theta$$

$$w_2 = -u_1 \sin \theta + w_1 \cos \theta \tag{31}$$

$$v_2 = v_1$$

Orientation stereogram. Probe pitched down by θ, yawed by ϕ and rolled by ρ.

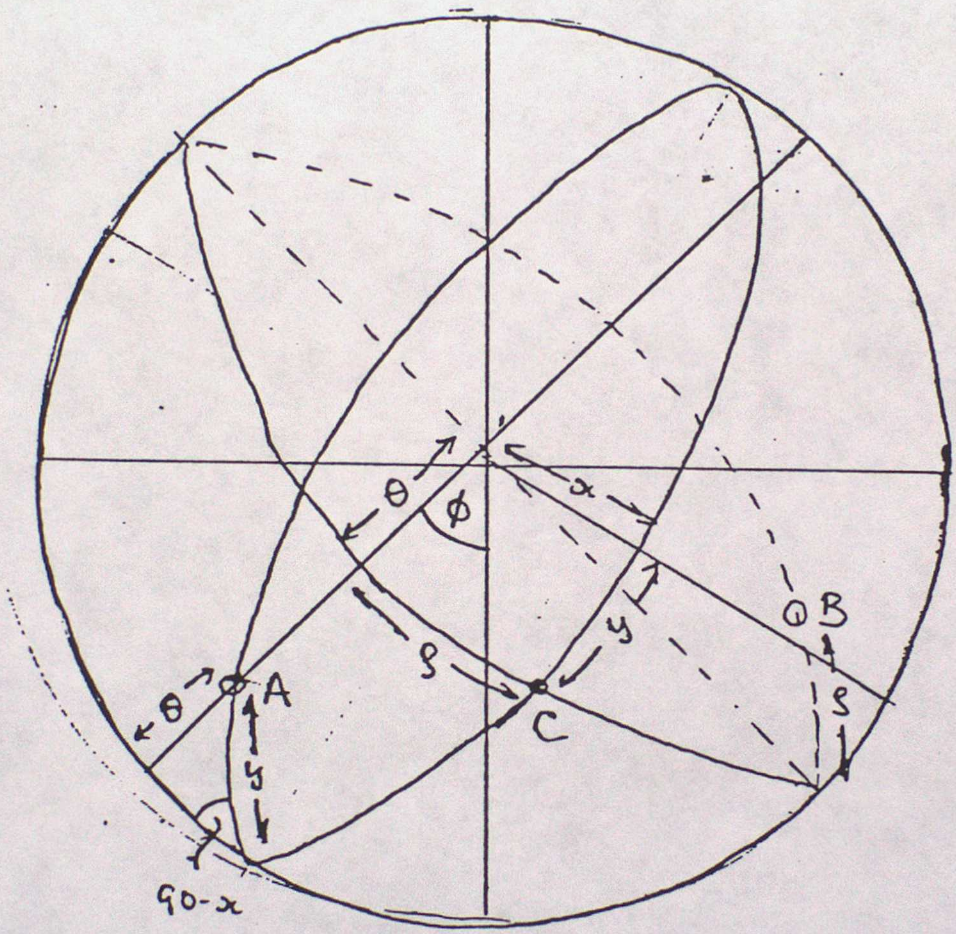

Figure 3: Stereographic projection: circles show north pole projection (vectors below plane of unit circle), dots south pole projection (vectors above plane of unit circle). A is probe fore-aft axis, B port-starboard axis, and C cable (up-down) axis.

(iii)

$$u = u_2 \cos\phi + v_2 \sin\phi$$
$$v = -u_2 \sin\phi + v_2 \cos\phi \tag{32}$$
$$w = w_2$$

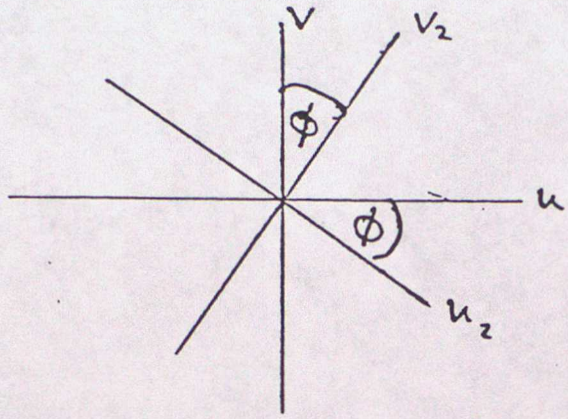

$$u_2 = u_1 \cos\theta + w_1 \sin\theta \tag{33}$$

$$u_2 = u' \cos\theta + \sin\theta(-v' \sin\rho + w' \cos\rho) \tag{34}$$

$$w_2 = -u_1 \sin\theta + w_1 \cos\theta \tag{35}$$

$$w_2 = -u' \sin\theta + \cos\theta(-v' \sin\rho + w' \cos\rho) \tag{36}$$

$$v_2 = v_1 \tag{37}$$

$$v_2 = v' \cos\rho + w' \sin\rho \tag{38}$$

$$u = u_2 \cos\phi + v_2 \sin\phi \tag{39}$$

$$u = (u' \cos\theta + \sin\theta(-v' \sin\rho + w' \cos\rho)) \cos\phi + (v' \cos\rho + w' \sin\rho) \sin\phi \tag{40}$$

$$v = -u_2 \sin\phi + v_2 \cos\phi \tag{41}$$

$$v = -\sin\phi(u'\cos\theta + \sin\theta(-v'\sin\rho + w'\cos\rho)) + (v'\cos\rho + w'\sin\rho)\cos\phi \tag{42}$$

$$w = w_2 \tag{43}$$

$$w = -u'\sin\theta + \cos\theta(-v'\sin\rho + w'\cos\rho) \tag{44}$$

where (see back)

$$\sin\theta = -a/g \quad \cos\theta = P/g \tag{45}$$

$$\sin\rho = b/P \quad \cos\rho = Q/P \tag{46}$$

$$\cos\phi = \frac{g\alpha - H_z a}{H_x P} \tag{47}$$

$$\sin\phi = \frac{g\beta P^2 + ab\alpha - H_z bg}{H_x PQ} \tag{48}$$

defining

$$P = \sqrt{(g^2 - a^2)}, Q = \sqrt{(g^2 - a^2 - b^2)} \tag{49}$$

Hence substituting for sines and cosines of ρ, θ, ϕ:

$$u = \left[\frac{u'P}{g} + \frac{a}{g}\left(-\frac{v'b}{P} + \frac{w'Q}{P}\right)\right]\left[\frac{g\alpha - H_z a}{H_x P}\right] + \left(\frac{v'Q}{P} + \frac{w'b}{P}\right)\left[\frac{\beta P^2 + ab\alpha - H_z bg}{H_x PQ}\right] \tag{50}$$

$$v = \left[\frac{u'P}{g} + \frac{a}{g}\left(-\frac{v'b}{P} + \frac{w'Q}{P}\right)\right]\left[-\frac{(\beta P^2 + ab\alpha - H_z bg)}{H_x PQ}\right] + \left(\frac{v'Q}{P} + \frac{w'b}{P}\right)\left[\frac{g\alpha - H_z a}{H_x P}\right] \tag{51}$$

$$w = -\frac{u'a}{g} + \frac{P}{g}\left(-\frac{v'b}{P} + \frac{w'Q}{P}\right) \tag{52}$$

If we make

$$a = a/g, b = b/g, \alpha = \alpha/H, \beta = \beta/H \tag{53}$$

$$H_z = H_z/H, H_x = H_x/H, P = \sqrt{1 - a^2/g_2} \tag{54}$$

$$\text{and } Q = \sqrt{1 - a^2/g^2 - b^2/g^2} \tag{55}$$

this reduces to the following transformation matrix:

$$\begin{pmatrix} (\alpha - H_z a)/H_x & (\beta - bH_z)/H_x & [b\beta + a\alpha - H_z(a^2+b^2)]/H_x Q \\ (-ab\alpha + H_z b - \beta P^2)/H_x Q & (\alpha - H_z a - b^2\alpha + ab\beta)/H_x Q & (-a\beta + b\alpha)/H_x \\ -a & -b & Q \end{pmatrix} \tag{56}$$

This should be applied to give:

$$[u, v, w] = [MATRIX] \begin{bmatrix} u' \\ v' \\ w' \end{bmatrix} \tag{57}$$

7 Inclinometers

The inclinometers should be given as ratios of voltage to maximum (90°) voltage — this will give $a/g, b/g$. The signs should be arranged to give positive θ and ρ as shown in the stereogram ie. θ positive pitching down, ρ positive port side down. Their zeroes should be set by an initial vertical calibration. The inclinometers can suffer from high frequency "noise" due to cable vibrations and bearing rattle which may be removed by pre-filtering.

8 Magnetometers

Their readings should be given as ratios of voltage to maximum voltage. The maximum voltage can be taken as the sums of the squares of the individual voltages, i.e.

$$V_\alpha/V_H = V_\alpha/\surd(V_\alpha^2 + V_\beta^2 + V_\gamma^2) = \alpha/H \tag{58}$$

The signs of α, β are such that pointing either the nose (for α) or the port side of the probe (for β) north gives positive readings. The angle of dip must be measured or known to give H_x/H and H_z/H. In theory it may be determined from the redundant relation

$$\cos^2\phi + \sin^2\phi = 1 \tag{59}$$

i.e.

$$(g\alpha - H_z a)^2 + [\beta(g^2 - a^2) + ab\alpha H_z bg]^2/(g^2 - a^2 - b^2) = H_x^2(g^2 - a^2) \tag{60}$$

9 Rotation into the mean wind

The wind vectors obtained from the probe are referenced to a right handed orthogonal set of North, West, Up (u, v, w respectively). In order to rotate into the mean wind the average values of u, v, w are first obtained. These are then rotated as follows:

$$\theta_{uv} = \tan^{-1}(\bar{v}, \bar{u}) \tag{61}$$

$$\theta_w = \tan^{-1}(\overline{w}, \sqrt{(\overline{u}^2 + \overline{v}^2 + \overline{w}^2)}) \tag{62}$$

$$u'' = u \cos\theta_{uv} + v \sin\theta_{uv} \tag{63}$$

$$v' = v \cos\theta_{uv} - u \sin\theta_{uv} \tag{64}$$

$$u' = u'' \cos\theta_w = w \sin\theta_w \tag{65}$$

$$w' = w \cos\theta_w - u'' \sin\theta_w \tag{66}$$

It should be noted that although the mean value system u', v', w' are self defined in the u' direction, there is an ambiguity between v' and w' that depends on the original u, v, w axes being correctly oriented with respect to gravity. Thus the inclinometers must be correctly zeroed to avoid false cross correlations between v and w. Finally it should be noted that in deriving the wind direction (D):

$$D = \tan^{-1}(-v/u) + 180° \tag{67}$$

where v is measured westward, u northward.

10 Calculation of the dip angle

Large errors in mean and turbulence quantities can occur if a dip angle is imposed that is not consistent with the probe measured values of magnetic field and inclination. The mean value errors are 5% per degree error and the effect on turbulence quantities is worse. It has been found that provided the self measured dip angle is used the data is partially free from magnetometer calibration and mounting errors.

Assuming the components of the earths field H_x and H_z have been normalised using all three magnetometer readings so that $H_x^2 + H_z^2 = 1$. Then taking components along the vertical:

$$H_z = \alpha \sin\theta - \cos\theta(\gamma \cos\rho - \beta \sin\rho) \tag{68}$$

$$H_z = a\alpha - \gamma - \gamma Q + \beta b \tag{69}$$

where

$$Q = \sqrt{(1 - a^2 - b^2)} \tag{70}$$

Then

$$H_x = \sqrt{(1 - H_z^2)} \tag{71}$$

$$\text{Dip angle} = \tan^{-1}[H_z/\sqrt{(1 - H_z^2)}] \tag{72}$$

This measurement essentially uses the extra information provided by the redundancy relation:

$$(\alpha - H_z a)^2 + \frac{\beta(1 - a^2) + ab\alpha - H_z b}{1 - a^2 - b^2} = H_x^2(1 - a^2) \tag{73}$$

This can be treated as a quadratic in H, the solution of which is:

$$H_z = a\alpha + \beta b \pm \gamma Q \tag{74}$$

10.1 Separate calculation of horizontal mean wind — a check

We now describe how to measure the mean wind component parallel to the probe in the horizontal plane *from each Gill independently*, assuming probe is lined up parallel to the wind. This is a useful probe diagnostic as it is independent of magnetometer measurements and checks each Gill separately.

Using the probe stereogram, the angle y between the probe tail axis and the intersection between the probe tail - cable axis and the horizontal is first found:

$$\sin y = \frac{\sin\theta}{\cos x} \tag{75}$$

$$\cos x = \frac{\cos\theta\cos\rho}{\cos y} \tag{76}$$

$$\tan y = \frac{\tan\theta}{\cos\rho} = \frac{a}{P}\frac{P}{Q} = \frac{a}{Q} \tag{77}$$

Using the Gill stereogram, the three direction cosines between each of the three Gills and the horizontal vector parallel to the probe tail are then found.

For the top Gill this is

$$\cos(H - D - y) = \cos(H - D - \tan^{-1} a/Q) \tag{78}$$

For the port and starboard Gills this is:

$$\cos p \cos(r + D + y) \tag{79}$$

where

$$r = \cos^{-1}\left[\frac{\cos H}{\sqrt{1 - (3/4)\sin^2 H}}\right] \tag{80}$$

(giving $r = \cos^{-1} 2\sqrt{(3/13)}$ in the case $H = 30°$) and

$$y = \tan^{-1}(a/Q) \tag{81}$$

These direction cosines should then be corrected for Gill cosine error. The three mean winds parallel to the probe so derived will only be equal if the probe tail is correctly aligned. A consistent difference between mean winds calculated from port and starboard Gills indicates misalignment and in this case the top Gill reading will be incorrect.

11 Tracking

A possible method of tracking the balloon in order to determine the effect of balloon motions is to use the inclinometer, magnetometer and pressure sensor readings of probes mounted at several points on the cable. A piece wise fit may then be made to the cable curve using the derived probe orientations to find the co-ordinates of each probe and hence their translational velocities by differentiation.

The first step is to determine the azimuth and dip angles m and n of the probe axes using the pitch, roll, and yaw angles (θ, ρ, ϕ) determined in the previous section. It should be noted that the velocities of the probe relative to the ground due to balloon motions derived above should be *added* to the wind velocities u, v, w measured by the probe itself.

Using the tracking stereogram as follows:

$$\sin(90^\circ - \rho) = \frac{\sin(90^\circ - m)}{\sin(90^\circ - \theta)} \tag{82}$$

$$\cos m = \cos\rho\cos\theta \tag{83}$$

$$\frac{\sin(\phi - n)}{\sin\rho} = \frac{1}{\sin m} \tag{84}$$

$$\sin(\phi - n) = \frac{\sin\rho}{\sin m} \tag{85}$$

Also

$$\sin m = \frac{\sin d}{\cos(\phi - n)} \tag{86}$$

and

$$\cos\rho = \frac{\sin d}{\sin\theta} \tag{87}$$

From (52) and (53),

$$\cos(\phi - n) = \frac{\cos\rho\sin\theta}{\sin m} \tag{88}$$

From the previous section:

$$\sin\theta = a, \cos\theta = P \tag{89}$$

$$\sin\rho = b/P, \cos\rho = Q/P \tag{90}$$

$$\sin\phi = \frac{\beta P^2 + ab\alpha - H_z b}{H_x PQ} \tag{91}$$

$$\cos\phi = \frac{\alpha - H_z a}{H_x P} \tag{92}$$

using previous definitions of symbols.

Hence

$$\cos m = Q \tag{93}$$

As $0^\circ < m < 90^\circ$,

$$\tan m = +\sqrt{1 - Q^2}/Q \tag{94}$$

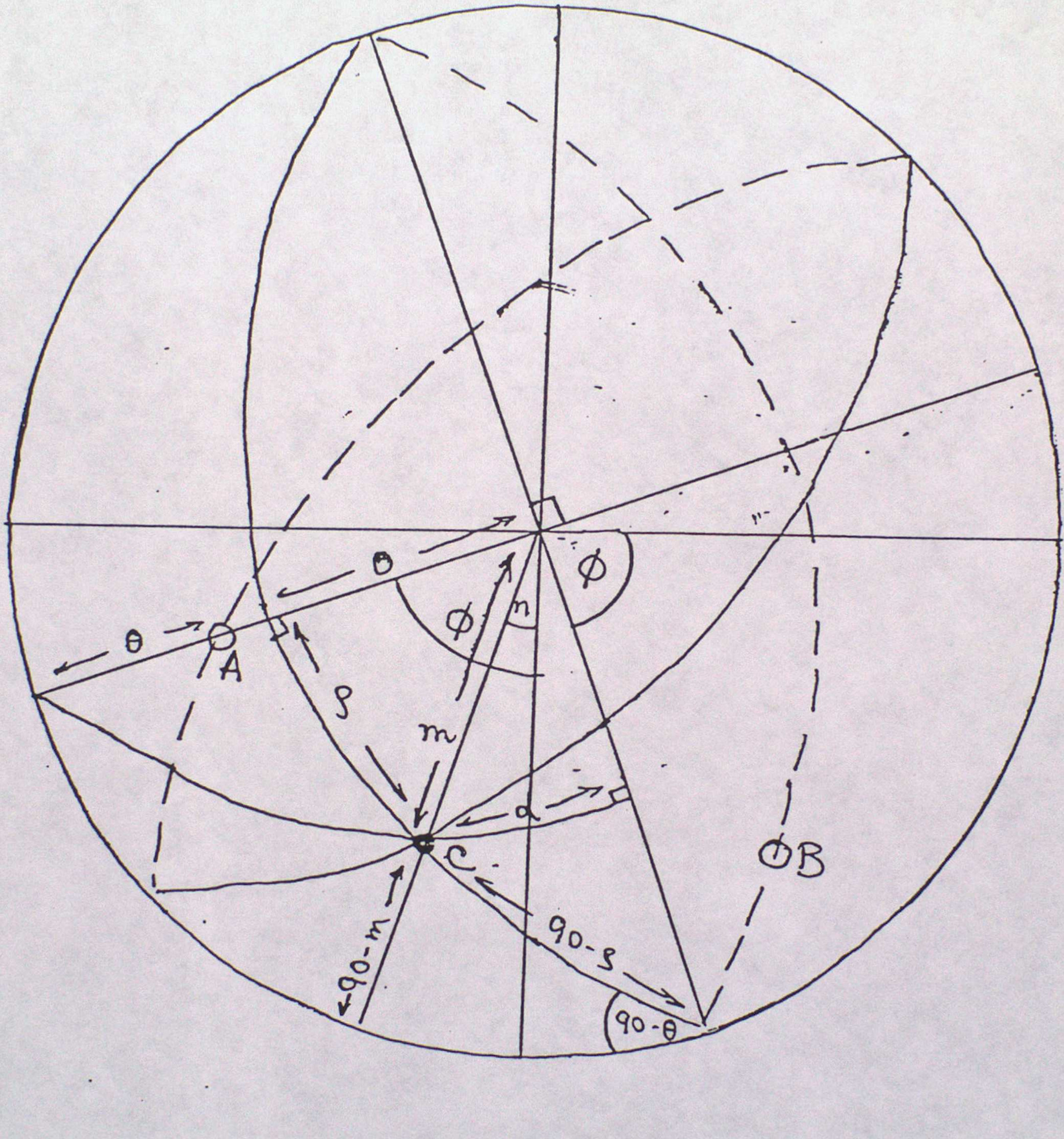

Figure 4: Tracking stereogram

$$\sin(\phi - n) = b/P\sqrt{1-Q^2} \tag{95}$$

$$\cos(\phi - n) = aQ/P\sqrt{1-Q^2} \tag{96}$$

$$-180^\circ < (\phi - n) \leq 180^\circ \tag{97}$$

$$\phi - n = \tan^{-1}(\cos(\phi - n), \sin(\phi - n)) \tag{98}$$

$$\phi = \tan^{-1}(\cos\phi, \sin\phi) \tag{99}$$

$$n = \phi - (\phi - n) \tag{100}$$

and will be in the range $-360^\circ < n < 360^\circ$. [Here by slight abuse of notation we have applied $\tan^{-1}$ to a vector, with the answer defined to be its direction.]

In fact $-180^\circ < n < 180^\circ$ and values outside this range can be shifted by adding or subtracting 360°.

Once m and n are uniquely determined at a point on the cable, they define the tangent to the cable at that point. A variety of approximations may then be used to determine the horizontal position of the probe relative to the pulley block, giving the probe height (z) above the pulling block. The simplest of these, used in the case of a single probe, assumes a straight cable.

Simple geometry gives:

Height $= z$

Northerly horizontal distance $= z \tan m \cos n$.

Westerly horizontal distance $= -z \tan m \sin n$.

These three distances need to be differentiated in order to obtain velocities for correcting to the probe determined velocities.

However differentiation of the unfiltered distances would produce a large contamination of the velocity power spectra at high frequencies due to the strongly frequency dependant effect of differentiation. A study must first be made of the spectra of the distances to determine the position of the peak due to balloon motions. Filtering (with cut-off period 30 secs) can then be applied to the distances to eliminate frequencies greater than this prior to differentiation. A simple catenary approximation neglecting effects of the wind on the cable, the weight of the probe and accelerations of the cable gives practically identical results to the linear approximation. This is presumably because both simple catenary and linear approximations are identical in their treatment of cable v motion which predominates and are similar for u motions as differentials are involved. Non-simple effects are probably at high enough frequencies to be eliminated by the filter.

12 Calculation of probe orientation using azimuth and declination angles together with magnetometer information

The peak in the inclinometer spectra due to non-gravitational accelerations induced by transverse cable vibrations occurs in a region of the spectrum where there is a significant contribution due to real probe motions. Filtering of the inclinometer spectra in this region will thus remove real information. However if the declination and azimuth angles m and n are first calculated as in the previous section then functions of these variables can be constructed that should only vary on the timescale of the balloon motions, which is an order of magnitude greater than the timescale of the probe motions. If these functions are filtered and m and n recalculated, then magnetometer data alone, which is not affected by accelerations, can be used to calculate the probe orientations. It should be noted that m cannot be directly filtered, as a time series of m varies as a square function during simple inverse pendulum motions of the balloon and filtering of this at short wavelengths would create spurious long wavelength v motions. Initially the functions $\tan m \sin n$, $\sin m \cos n$ were used but in highly turbulent conditions with large inclinometer readings extreme values of $\tan m$ gave singularities in the filtered function. Suitable functions for filtering are:

(i) $\sin m \sin n$

(ii) $\sin m \cos n$

which are components of the cable axial vector and are related to horizontal position.

It should be noted that a disadvantage of this method is the singularity that occurs when the probe is oriented along the magnetic axis. A careful check has to be made that the probe is never nearer than a few degrees of this orientation as digitization noise in the magnetometer chanel will begin to affect the spectra.

The following calculation assumes that m and n are available having been calculated as shown in the previous section and filtered as described above.

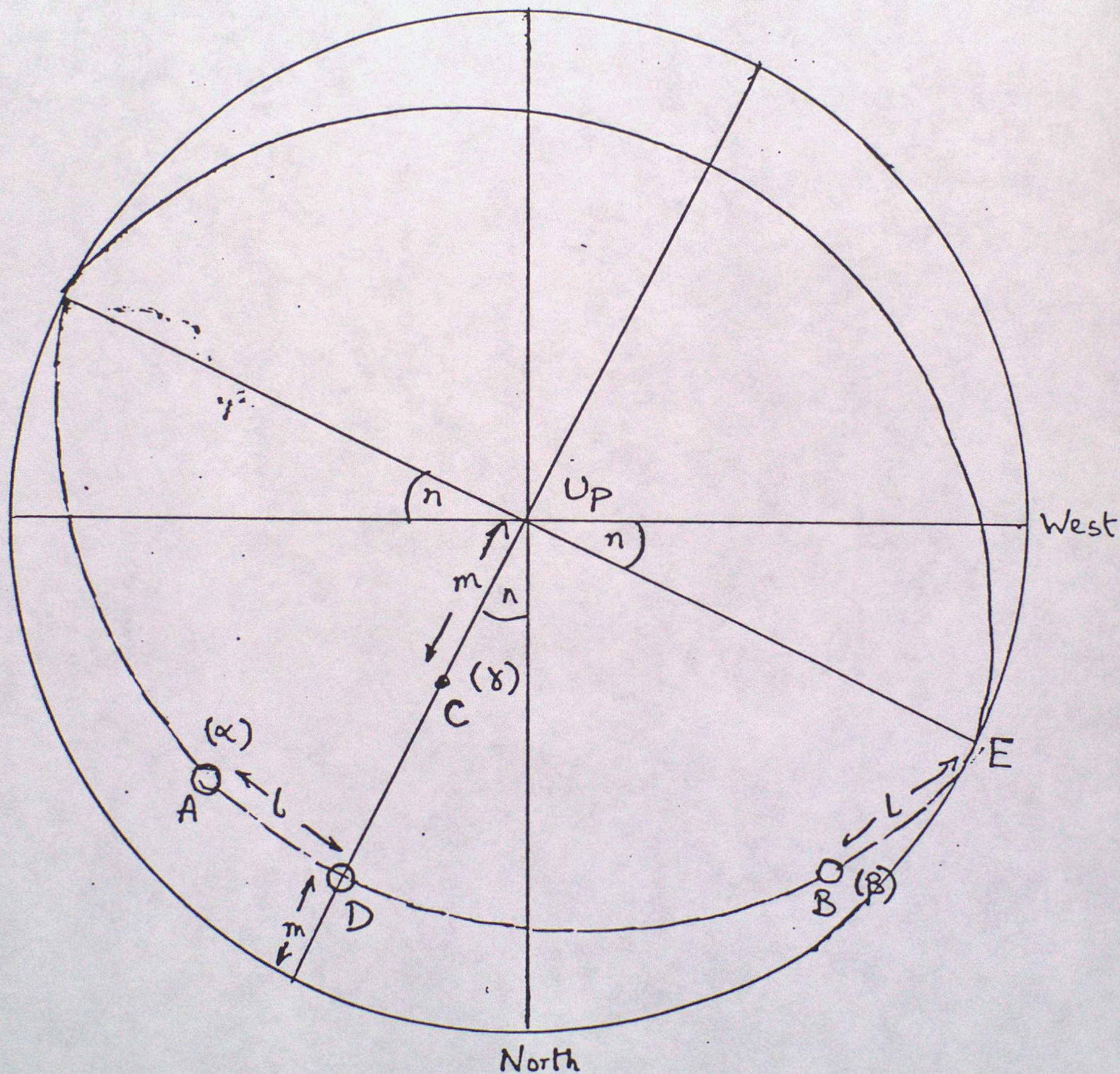

The probe x, y, z axes are A, B and C respectively. If magnetic field components are taken along C, D and E: which are the axes of the tilted but unrotated probe then:

$$\delta = H_x \cos n \sin m - H_z \cos m \tag{101}$$

$$\alpha \cos l + \beta \sin l = H_x \cos n \cos m + H_z \sin m \tag{102}$$

$$-\alpha \sin l + \beta \cos l = H_x \sin n \tag{103}$$

From the last two equations:

$$\sin l = \frac{\beta(H_x \cos n \cos m + H_z \sin m) - \alpha H_x \sin n}{\alpha^2 + \beta^2} \tag{104}$$

$$\cos l = \frac{\alpha(H_x \cos n \cos m + H_z \sin m) + \beta H_x \sin n}{\alpha^2 + \beta^2} \tag{105}$$

In the initial calculations of m and n, H was determined using the formula:

$$H_z = a\alpha + b\beta - \gamma\sqrt{1 - a^2 - b^2} \tag{106}$$

However for the calculation of $\sin l$ and $\cos l$ in the above formulae it must be redetermined as follows using filtered values m and n:

$$\gamma = H_x \cos n \sin m - H_z \cos m \tag{107}$$

whence, again, using the normalization

$$H_x^2 + H_z^2 = 1 \tag{108}$$

$$H_z = \frac{-\gamma \cos m \pm \cos n \sin m \sqrt{(\cos^2 n + \cos^2 n \sin^2 m - \gamma^2)}}{\cos^2 m + \cos^2 n \sin^2 m} \tag{109}$$

Unfortunately the sign to be used in this formula varies with m and n. The term within the square root defines a plane including the magnetic vector and the east - west direction: If the cable axis is north of this plane (the normal case) the position sign is used, otherwise the negative sign is used. As this formula is used to define the magnetic axis, it is not possible to determine if the cable axis is, in fact, north or south of the plane except using H_z defined as previous from inclinometer data. This has the disadvantage that H_z is not then fully compatible with the set of equations above, but is the only thing that can be done when the cable is laid back in a southerly direction. The north - south lay back angle is given by

$$\cos A = \frac{\cos m}{\sqrt{1 - \sin^2 m \sin^2 n}} \tag{110}$$

where A is positive for $\cos n > 0$ and negative for $\cos n < 0$

13 Rotation

The calculated values of $\sin l$, $\cos l$, $\sin m$, $\cos n$, $\cos n$ can now be used to determine the rotation matrix. These are three rotations:

Rotation about C axis gives:

$$u' = u\cos l + \sin l \tag{111}$$

$$v' = -u\sin l + v\cos l \tag{112}$$

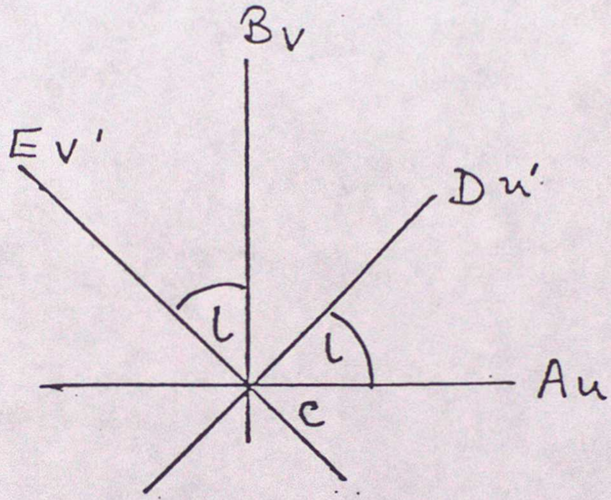

Rotation about E axis gives:

$$u'' = u'\cos m + \sin m \tag{113}$$

$$w'' = -u'\sin m + w\cos m \tag{114}$$

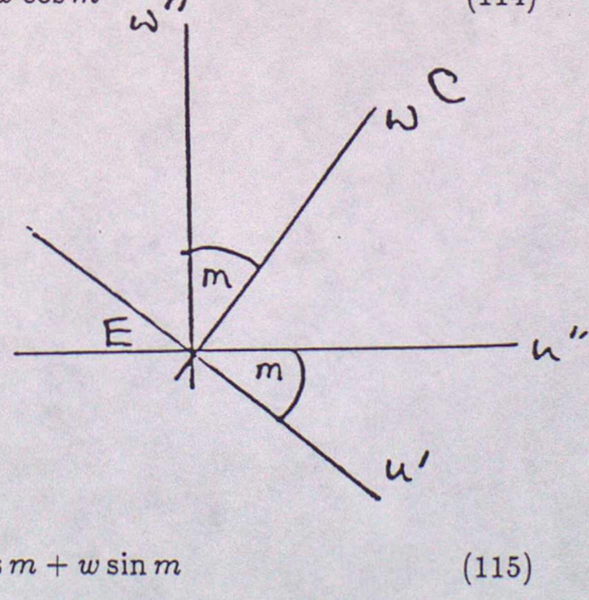

$$u'' = (u\cos l + v\sin l)\cos m + w\sin m \tag{115}$$

$$w'' = -(u\cos l + v\sin l)\sin m + w\cos m \tag{116}$$

Rotation about vertical axis gives:

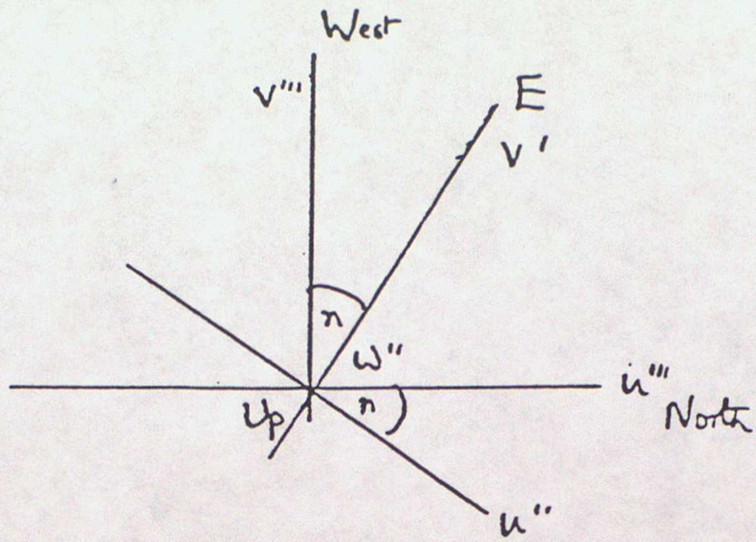

$$u''' = u'' \cos n + v' \sin n \tag{117}$$

$$v''' = -n'' \sin n = v' \cos n \tag{118}$$

$$w''' = w'' \tag{119}$$

Hence the rotation matrix M is:

$$\begin{pmatrix} \cos l \cos m \cos n - \sin l \sin n & \sin l \cos m \cos n + \cos l \sin n & \sin m \cos n \\ -\cos l \cos m \sin n - \sin l \cos n & -\sin l \cos m \sin n + \cos l \cos n & -\sin m \sin n \\ -\cos l \sin m & -\sin l \sin m & \cos m \end{pmatrix} \tag{120}$$

where

$$\underline{\mathbf{u}} \begin{bmatrix} North \\ West \\ Up \end{bmatrix} = \begin{bmatrix} MATRIX \end{bmatrix} \times \ \underline{\mathbf{u}} \begin{bmatrix} Turbulence \\ Probe \\ axes \end{bmatrix} \tag{121}$$

14 Accelerometer Corrections

Provided that the balloon induced motions of the cable are well seperated in frequency from other cable motions then the orientation of the cable is well defined to within the period of the balloon motion. In this case magnetometer data alone is required to give the rotation of the probe about the cable and any inclinometer angle that is not campatible with the orientation angle so derived can be assumed to be due to accelerations. These accelerations can be interested to give sideways cable velocities and used to correct for 'twanging' modes of the cable. If a and b are the inclinometer readings, and m, n,and l are defined as previously

Acceleration in 'n' direction:

$$A_n = s(a \sin l + b \cos l - \sin m) \tag{122}$$

Acceleration in 'm' direction:

$$A_m = g(a\cos l - b\sin l) \tag{123}$$

Where g is the acceleration due to gravity.

Then in north, west up frame:

$$A_{north} = A_n \sin n + A_m \cos m \cos n \tag{124}$$

$$A_{west} = A_n \cos n - A_m \cos m \sin n \tag{125}$$

$$A_{up} = -A_m \sin m \tag{126}$$

A_{up} is not used as it is incomplete, there being no 'z' inclinometer

This can now be integrated: $V_t = V_{t-1} - \Delta t A$ where V is velocity at time t, V_{t-1} at time $t-1, \Delta t$ is the time internal, and A is the acceleration.

The boundary conditions used is derived from the fact that the probe dosen't go anywhere. Hence the mean position doesn't change, and the mean velocity is therefore zero. Therefore the mean velocity determined by the calculations is set to zero by subtraction.

In practice this system has large drifts, but these can be subtracted off to give useful information. In fact in a perfect system no motion can occur on a timescale greater than the balloon motion period as the mean probe accelerations are assumed zero on this timescale in deriving the probe orientation. This assumption is not fully justified and is sometimes seriously in error but has to be used in this calculation. Therefore the inclinometer derived velocities are hi-pass filtered on the timescale of the balloon motions and the resultant velocities added (not subtracted) to the probe measured gusts as in the case of the balloon motion correction.

15 Correction of Gill frequency response

The arrangement of length constants resulted in the higher frequency direction variations being measured by the Gill anemometers, while the lower frequencies were measured through the package attitude. The length scale of the package response to rotation about the cable Lp was about 3m and fairly close to the length constant Lg(about 1m) of the Gills. As a result the measurement of turbulence at wavelengths of the order of Lp and in the "transition" region was affected to a some degree by the amplitude and phase response of the Gill anemometers. If this amplitude and phase response is not corrected for, then the two sources of information on the direction of the flow do not match and the combined direction information shows a spurious increase in variance in this frequency range. In fact, even with corrections, the velocities derived from the Gills will have some errors due to inaccuracies in both the cosine corrections, and the phase and amplitude response corrections. Because of this a residual error at wavelengths of the order of 2πLp is inevitable. The error is mainly confined to the lateral velocity component (v-component) and the energy spectrum of this component tends to show a peak. In order to assess the size of the above error quantitatively, the frequency response of the vane due to a forcing oscillation in the lateral wind has to be studied. A wind vane has a second order response, and its transfer function rises from a value of unity at low frequencies to a maximum at a wavelength of the order of 2πLp (see e.g. Busch et al. 1980). When mounted on a cable the turbulence probe has a peak value of its transfer function of about 1·8 at a wavelength of 16 metres, and the value falls to its half power point at a wavelength of 8 metres. At wavelengths around $2\pi\lambda_p$, the phase lag between the probe vane and the forcing oscillation is 90°, and thus the Gills experience an airflow which is the combination of two components, one 1·8 times the other in amplitude with a phase lag of 90°. The resultant is 2 times the amplitude of the forcing oscillation and has a phase lag of 30° with respect to it. This result has been derived by comparing the lateral velocity information obtained from the Gill anemometers and from the vane orientation separately, with results obtained from a nearby ultra-sonic anemometer. In a typical case the lateral velocity variance obtained from the Gill anemometers alone, in the waveband of order Lp, is about 400% greater than that due to the forcing motions. Combination of the Gill derived velocities with the attitude derived velocities without regard for the phase and amplitude corrections reduces this excess to about 80%. Application of the Gill anemometer phase and amplitude corrections reduces the excess to about 25%. This residual value is due to both the errors involved in the combination and to other influences discussed below.

The amplitude and phase corrections were obtained by applying a simple first order algorithm to the Gill anemometer outputs i.e.

$$G(t) = Gm(t) + \tau(Gm(t+Dt) - Gm(t-Dt))/2Dt \tag{127}$$

where G(t) and Gm(t) are the corrected and measured Gill outputs respectively at time t, τ is the response time of the Gills, and Dt is the data interval. The response time τ was derived using measurements of the prevailing windspeed and a length constant of $L\sqrt{(\cos(\theta))}$ where θ is the angle of the Gill to the instantaneous wind and L has a value of 1 metre (Hicks B.B. 1972). This procedure is adequate to improve the response for turbulence length scales down to about 1m. For shorter scales there are problems with electrical noise and signal resolution which limit the accuracy. At these shorter scales electrical filters have been used to prevent aliasing errors and it is impossible to recover information. The above corrections for amplitude and phase response, and the correction for non-cosine response, are all interdependent and strictly speaking an iteration involving all procedures is required. In practice the results are quite insensitive to this interdependence and even a constant value of τ based on the mean wind speed and mean value of theta gives reasonable results. The procedure adopted is more refined than this and should be a little more accurate i.e. (i) apply the non-cosine correction to estimate the instantaneous value of theta and of the wind speed, then (ii) correct the raw data for the amplitude and phase response, and finally (iii) recalculate the non-cosine corrections. The phase corrections have only limited accuracy due to the frequency limit of the digitization rate, the uncertainties of the Gill anemometer length constant at large angles, and other factors. The non-cosine response corrections are made using an iterative procedure (Horst 1973) in which successive estimates are made of the true wind vector and tables give the measured angular response deviation. The corrected Gill measurements are converted into components of wind velocity relative to the probe frame of reference and then using the procedures discussed above they are converted into a fixed frame, and finally the cable motion corrections are applied.

16 Appendix: use of Stereograms

A stereogram is a two-dimensional representation of directions in 3-dimensions which is widely used in crystallography. First consider a sphere, the surface of which terminates the ends of vectors originating at the centre of the sphere. These ends, i.e. directions, are projected as points on the stereogram, which is defined as the plane through the centre of the sphere with points projected onto it towards the South pole. (This applies to 'Northern' points; Southern points are conventionally projected onto the plane towards the North pole and denoted by open circles.) These ends can be joined by curves corresponding to great circles on the sphere. A theorem of projective geometry (see McKie and McKie or Philips) says that great circles project onto arcs of circles on the stereogram. Three points can thus be joined as a triangle:

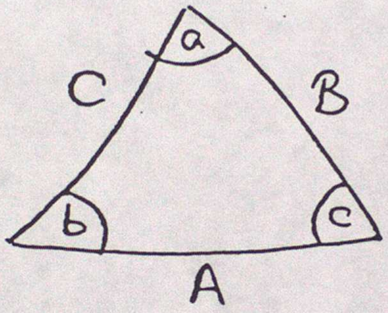

Note that A, B, and C are all angles subtended at the centre of the sphere by the vectors at the apices of the triangle.

The sine formula used in previous sections is:

$$\frac{\sin A}{\sin a} = \frac{\sin B}{\sin b} = \frac{\sin C}{\sin c} \tag{128}$$

This can be simplified in the case where *a, b or c* is a right angle. There is also a cosine formulae:

$$\cos a = \cos b \cos c + \sin a \sin b \cos c \tag{129}$$

which for a right angled triangle reduces to :

$$\cos a = \cos b \cos c \tag{130}$$

17 Notation

Acknowledgement

I would like to thank Mrs. G.Kimpton for typing up such a lot of maths and Steve Derbyshire for proof reading the results.

References

McKie, D. and McKie, C. (1974): Crystalline solids. Nelson, London. 628pp.

Philips - Elements of Crystallography (4th Edition).

Horst,T.W. (1973) Corrections for response errors in a three component propellor anemometer J.Appl.Met. Vol 12

Fig 1a

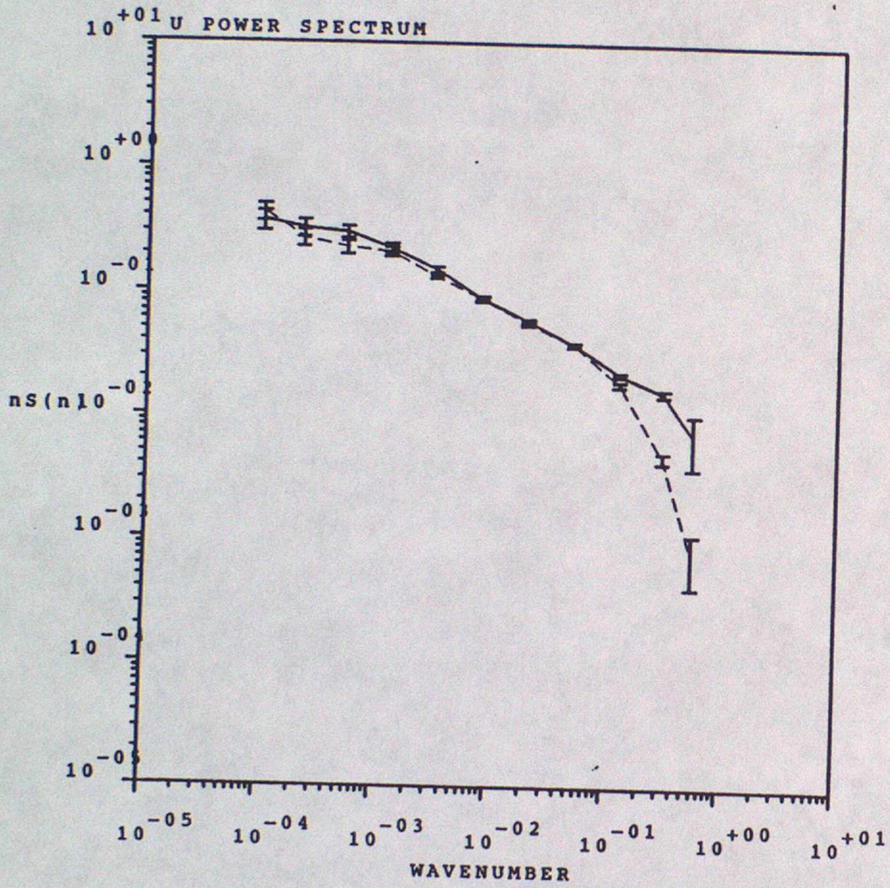
U POWER SPECTRUM
nS(n)
WAVENUMBER

Fig 1b

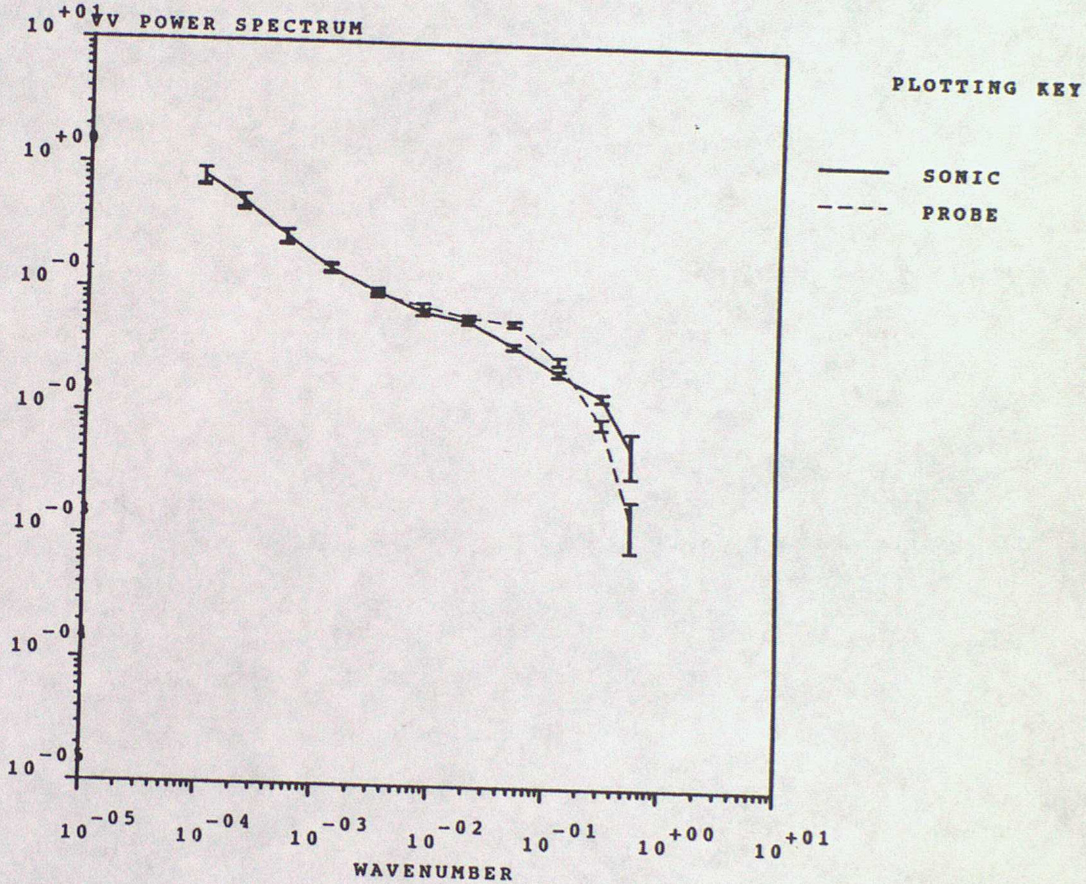
VV POWER SPECTRUM
WAVENUMBER
PLOTTING KEY
SONIC
PROBE

Fig 1c

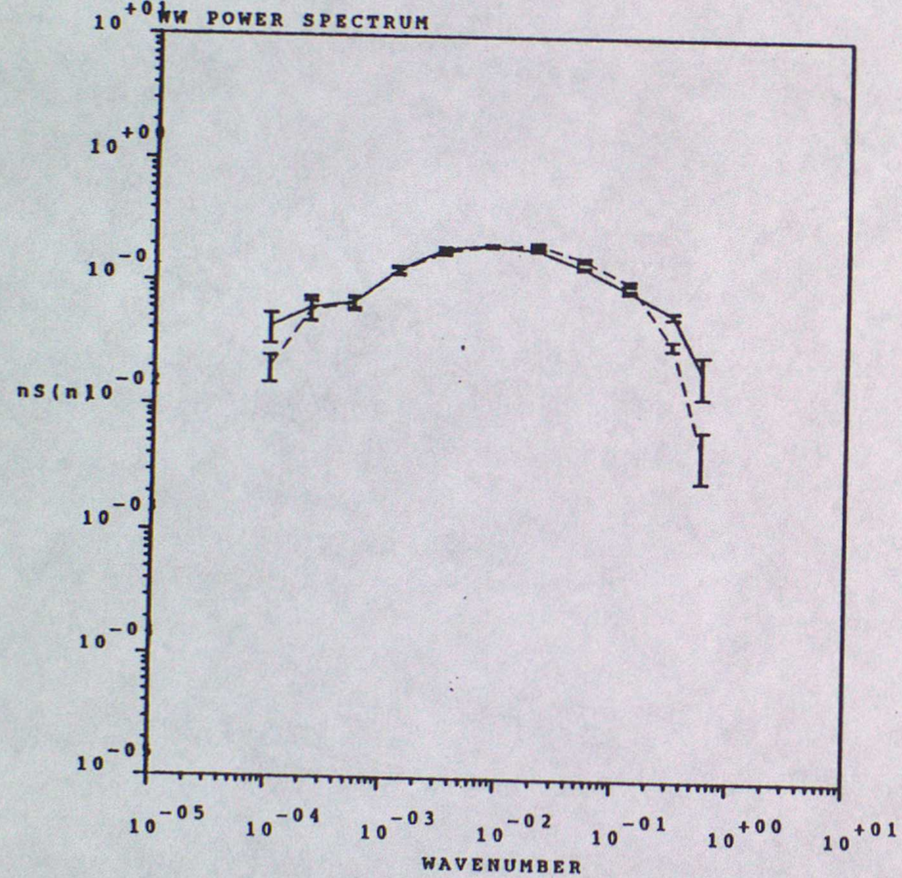
WW POWER SPECTRUM
nS(n)
10^+01
10^+00
10^-01
10^-02
10^-03
10^-04
10^-05
10^-05
10^-04
10^-03
10^-02
10^-01
10^+00
10^+01
WAVENUMBER

Fig 1d

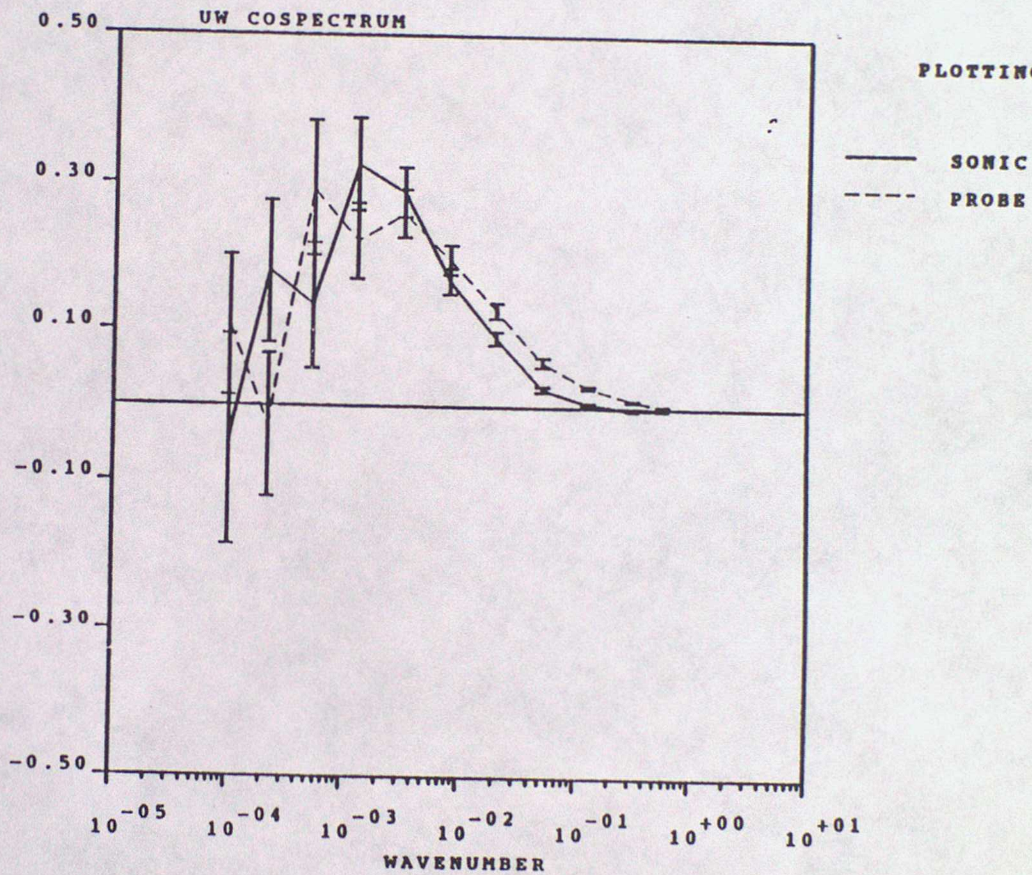
UW COSPECTRUM
0.50
0.30
0.10
-0.10
-0.30
-0.50
10^-05
10^-04
10^-03
10^-02
10^-01
10^+00
10^+01
WAVENUMBER
PLOTTING KEY
SONIC
PROBE

Fig (2)

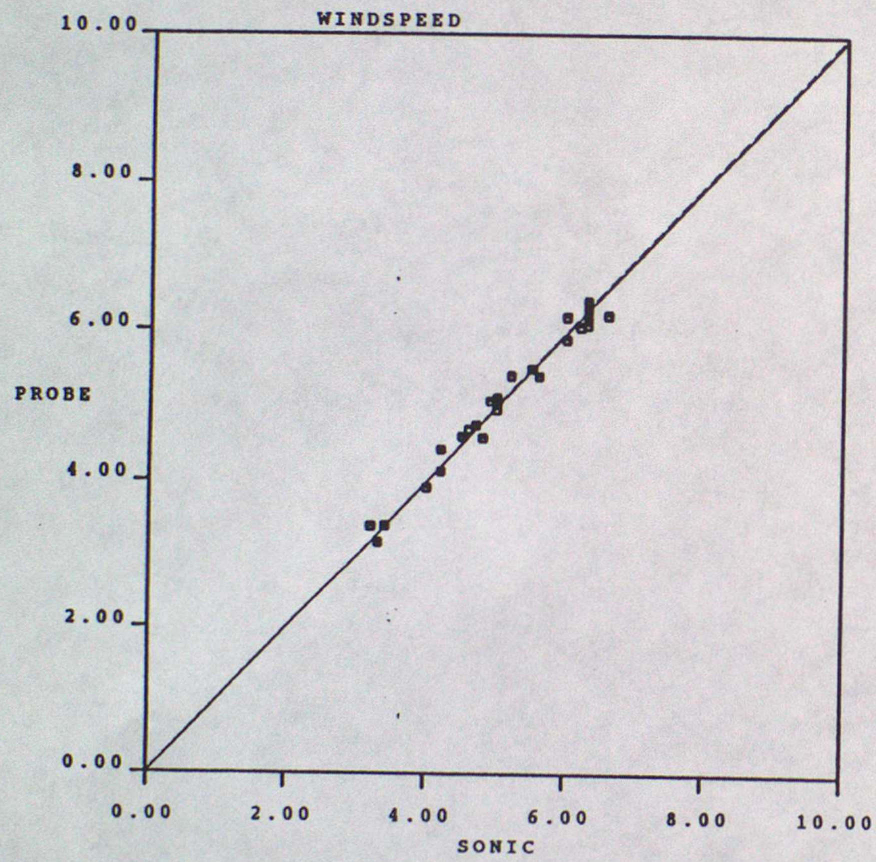

WINDSPEED
PROBE
SONIC
0.00
2.00
4.00
6.00
8.00
10.00

Fig 3a

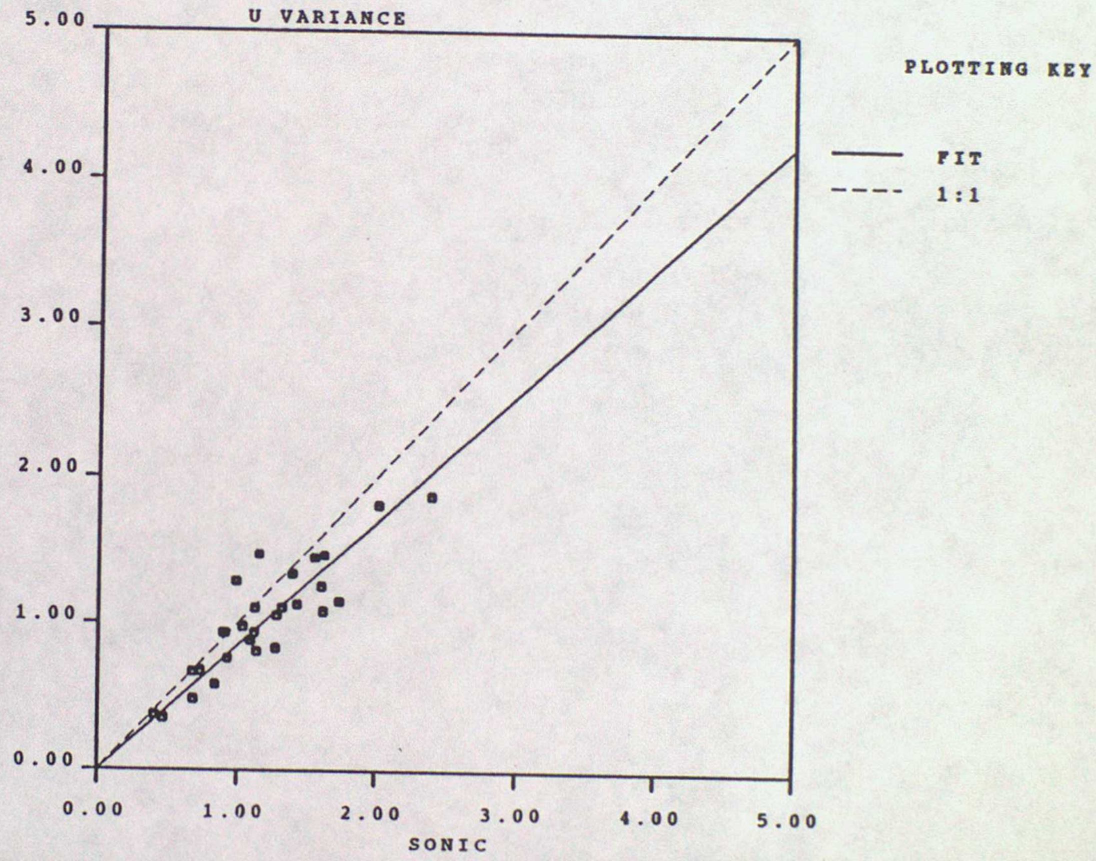

U VARIANCE
SONIC
0.00
1.00
2.00
3.00
4.00
5.00
PLOTTING KEY
FIT
1:1

Fig 3b

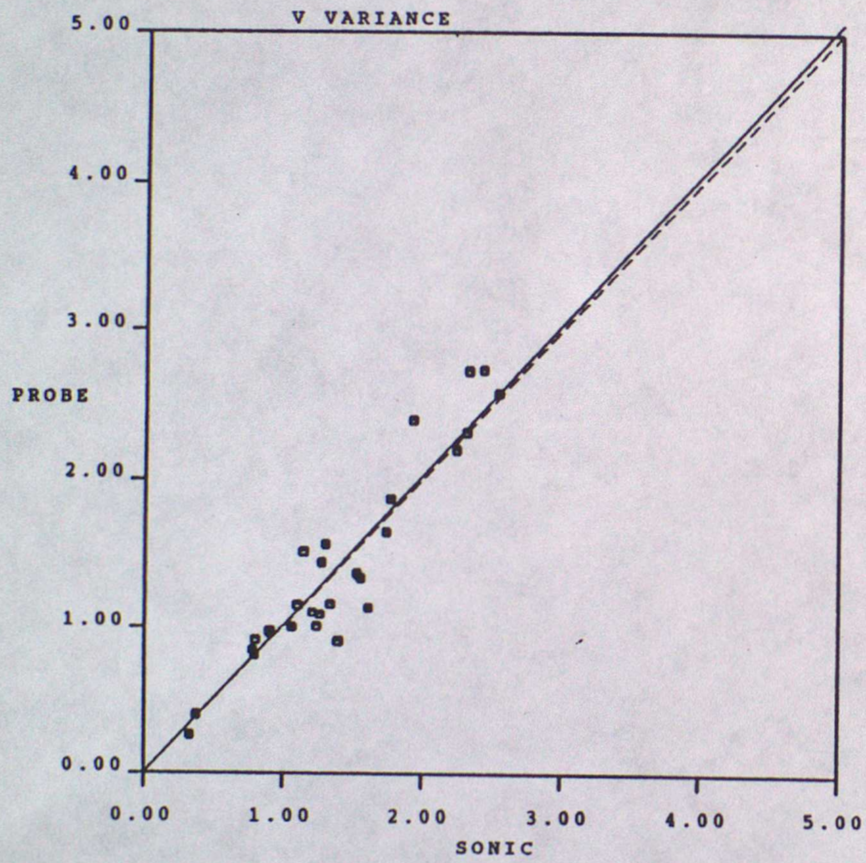
V VARIANCE
PROBE
5.00
4.00
3.00
2.00
1.00
0.00
0.00
1.00
2.00
3.00
4.00
5.00
SONIC

Fig 3c

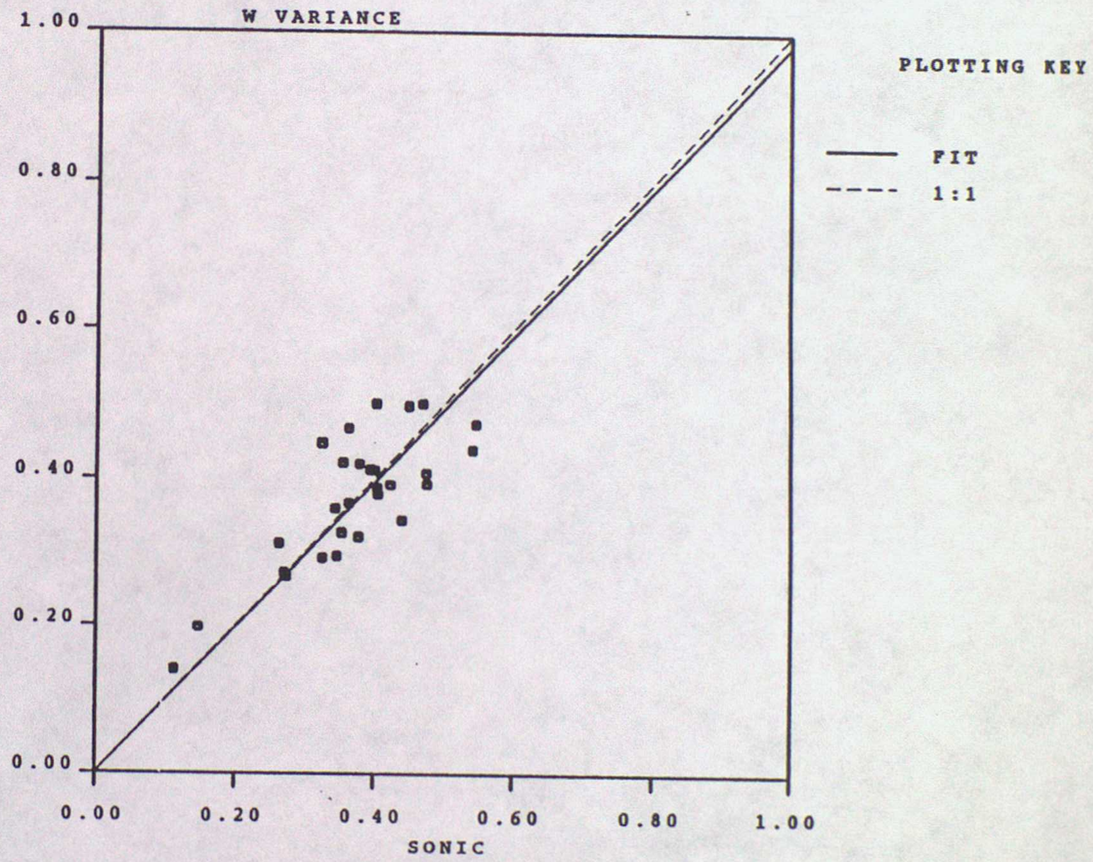
W VARIANCE
1.00
0.80
0.60
0.40
0.20
0.00
0.00
0.20
0.40
0.60
0.80
1.00
SONIC
PLOTTING KEY
FIT
1:1

Fig ~~3~~ 4

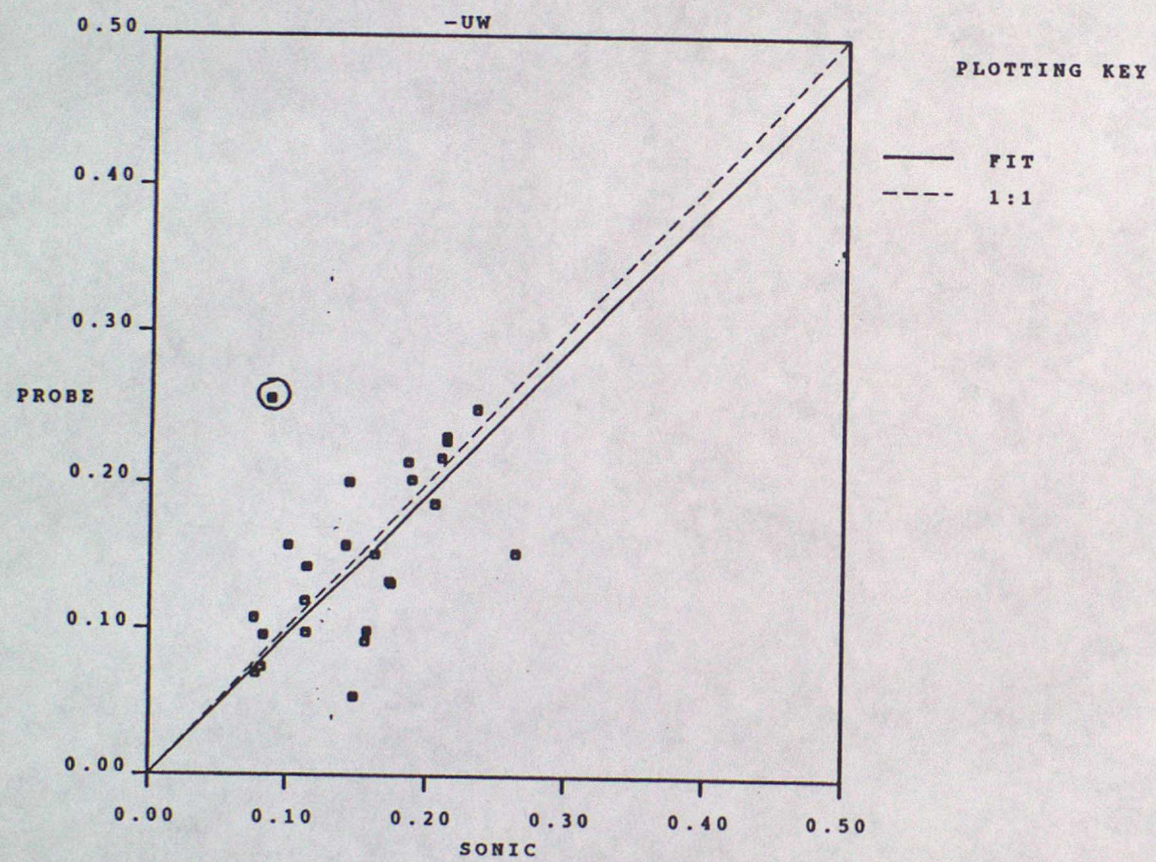
-UW
PROBE
0.50
0.40
0.30
0.20
0.10
0.00
0.00
0.10
0.20
0.30
0.40
0.50
SONIC
PLOTTING KEY
FIT
1:1

Fig 5a

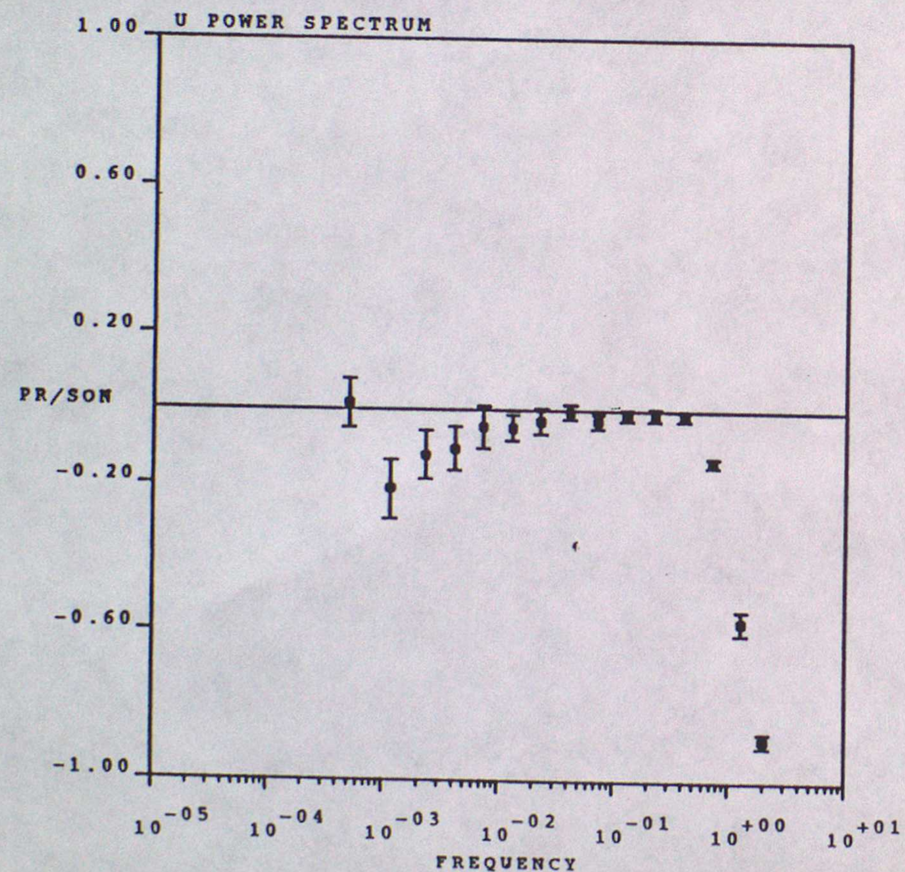
U POWER SPECTRUM
1.00
0.60
0.20
PR/SON
-0.20
-0.60
-1.00
10^{-05} 10^{-04} 10^{-03} 10^{-02} 10^{-01} 10^{+00} 10^{+01}
FREQUENCY

Fig 5b

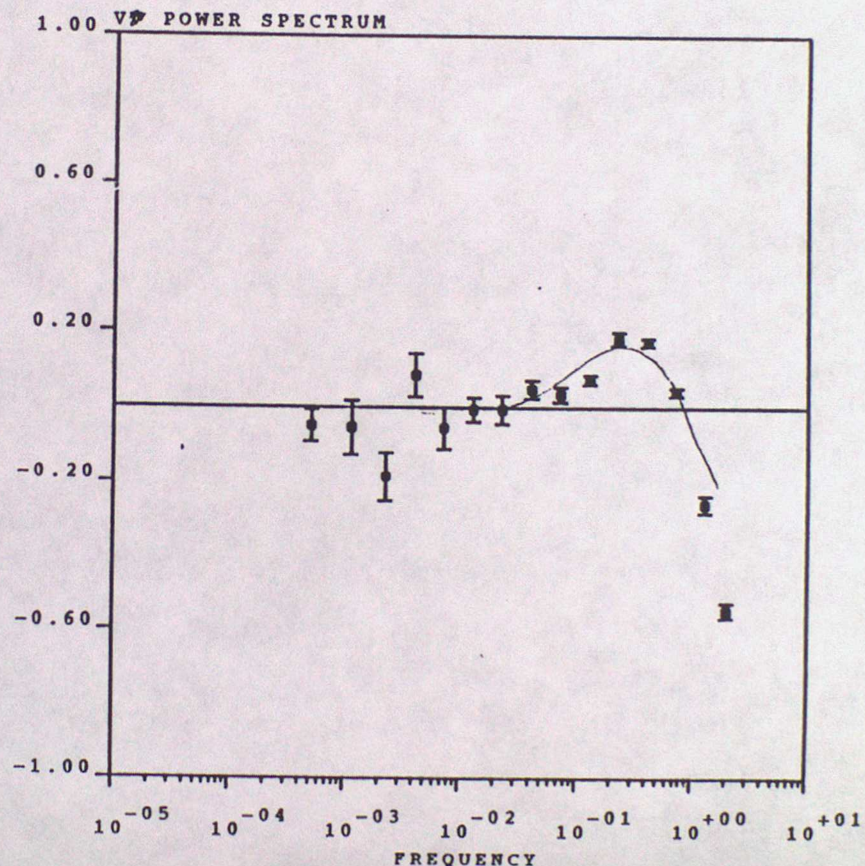
V POWER SPECTRUM
1.00
0.60
0.20
-0.20
-0.60
-1.00
10^{-05} 10^{-04} 10^{-03} 10^{-02} 10^{-01} 10^{+00} 10^{+01}
FREQUENCY

Fig 5c

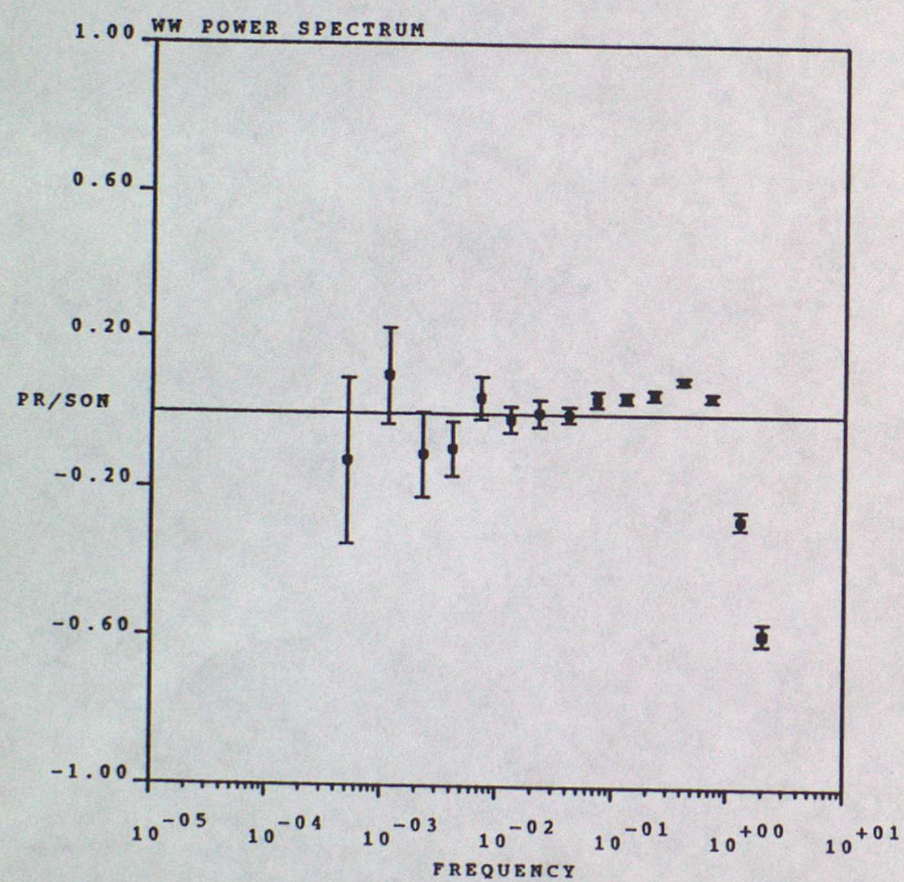
WW POWER SPECTRUM
1.00
0.60
0.20
PR/SON
-0.20
-0.60
-1.00
10^{-05}
10^{-04}
10^{-03}
10^{-02}
10^{-01}
10^{+00}
10^{+01}
FREQUENCY

Fig 5d

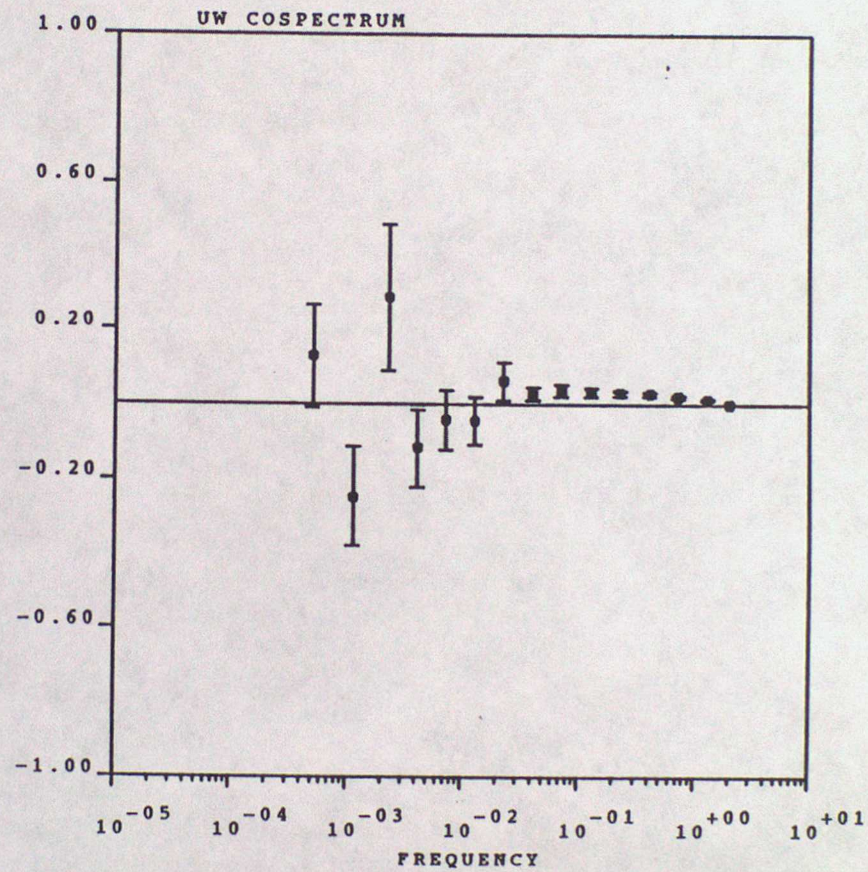
UW COSPECTRUM
1.00
0.60
0.20
-0.20
-0.60
-1.00
10^{-05}
10^{-04}
10^{-03}
10^{-02}
10^{-01}
10^{+00}
10^{+01}
FREQUENCY

Fig. 6a

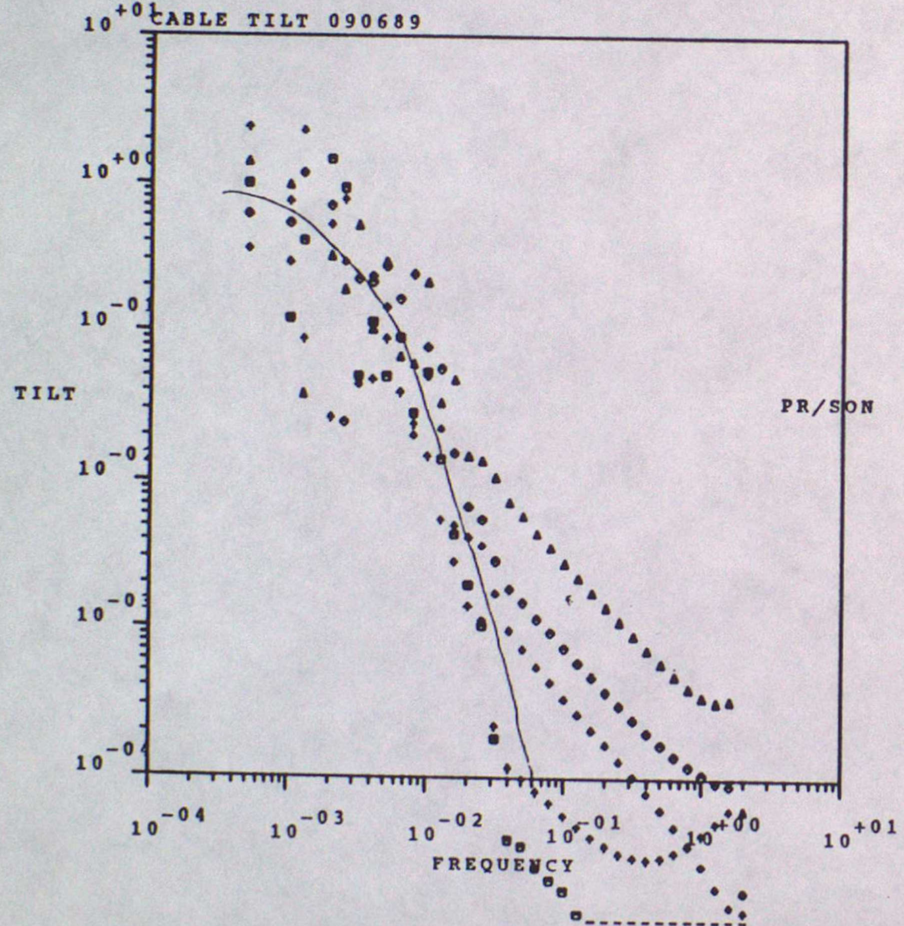

CABLE TILT 090689
TILT
FREQUENCY

Fig 6b

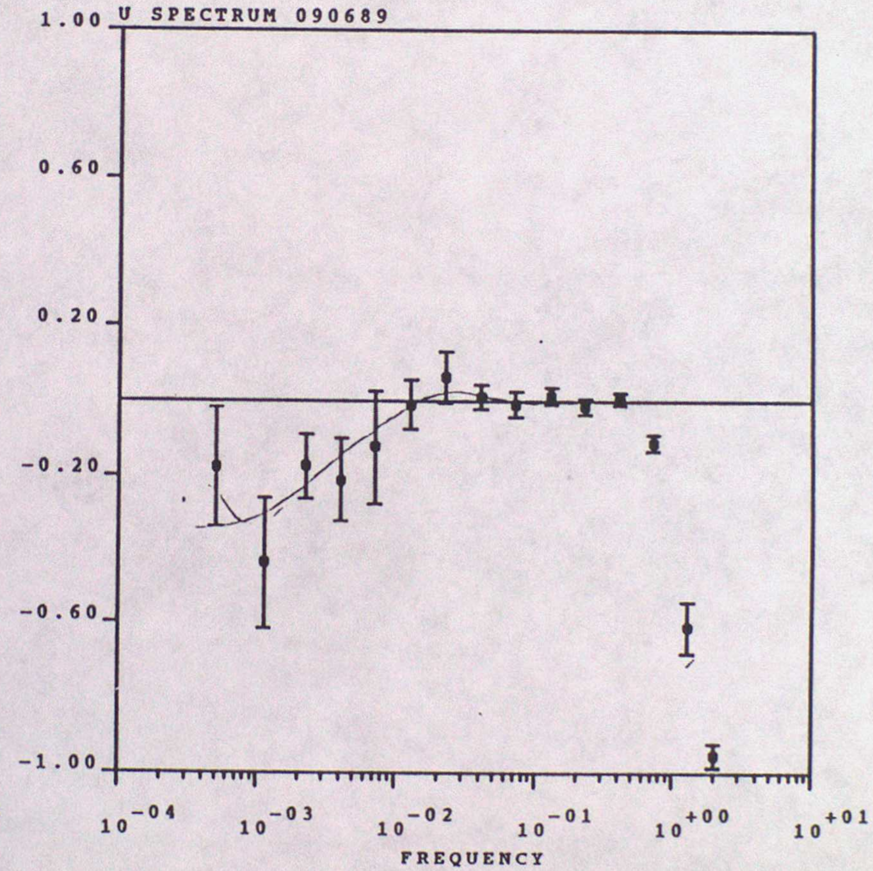

U SPECTRUM 090689
PR/SON
FREQUENCY